# Measurements, Analysis and Modeling of the Performance of Direct Detection Receivers with an Optical Preamplifier

by

Vikas Hari Butaney

Thesis submitted to the Faculty of the

Virginia Polytechnic Institute and State University

in partial fulfillment of the requirements for the degree of

**Master of Science**

in

**Electrical Engineering**

APPROVED:

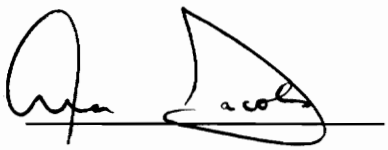

Dr. Ira Jacobs, Advisor

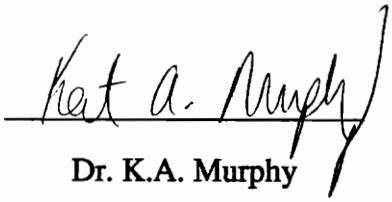

Dr. K.A. Murphy

Member of Committee

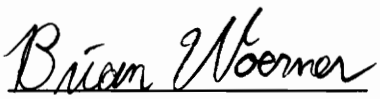

Dr. B. Woerner

Member of Committee

July, 1993

Blacksburg, Virginia

**Measurements, Analysis and Modeling of the Performance of Direct Detection Receivers with an Optical Preamplifier**

By

Vikas H. Butaney

Chairman of Committee: Dr. Ira Jacobs

Bradley Department of Electrical Engineering

In the last few years, erbium-doped fiber amplifiers (EDFAs) have been investigated extensively both for their superior amplification characteristics and their applicability to future optical fiber communication systems. In the preamplifier configuration, a bandpass filter is required to reduce the amplified spontaneous emission (ASE) noise in order to provide satisfactory bit error ratios (BER). In this thesis we examine the influence of the filter characteristics on performance. A model is derived to predict the BER performance of a preamplified APD receiver. The model is shown to be consistent with the experiments conducted at 2.5 Gb/s and data collected for various bandwidths and signal levels. The model is also compared with a recently published model, and the results show a good match. If the bandpass filter (BPF) has a small bandwidth and the laser center wavelength varies, the filter will attenuate the signal and introduce power penalties. The tradeoff between the stability of the system and the BER performance is presented, including experimental results for various bandwidths and offsets. It is shown that for optimal performance, a filter with a bandwidth about four times the expected variation in center wavelength should be used.

## ACKNOWLEDGMENTS

I would like to thank Dr. Jacobs for his guidance, motivation, and his continual support. His knowledge, and understanding of communications, electronics, and EM fields is not only awesome, its inspiring. I would also like to thank Dr. Murphy, and Dr. Woerner for their advice and suggestions.

I thank all the members of FEORC, who make FEORC an exciting, motivating, and a fun place to work.

I am grateful to my parents, Kamla & Hari Butaney, the most giving, open minded, and trusting parents. If it were not for them, I will not be who and where I am. I will like to thank my sister and brother-in-law Sujata & Rajiv Chainani for their support and encouragement through my education and maturing years. Lastly, I will like to thank Anjana Nagarajan, who helps me see the bigger picture, and continues to make my life exciting.

# TABLE OF CONTENTS

# LIST OF FIGURES

# LIST OF TABLES

## 1.0 INTRODUCTION

With present day optical transmitters and receivers, high speed optical communication links can typically extend to about 50 Km. But for trans-oceanic and longer distance terrestrial links, amplification of optical signals is required to provide satisfactory levels of performance. In the past 4-5 years erbium doped fiber amplifiers (EDFA) have grown from laboratory fascinations to practical and feasible components of long distance links. Unlike the previous generation of repeaters which convert the signal into electronic form before regeneration, EDFAs amplify light by directly multiplying or increasing the numbers of signal photons independent of data rates or modulation schemes. EDFAs have helped move present day communication systems closer to the dream of "universal information pipes", independent of information signals being transmitted or data rates being used, allowing users to dynamically multiplex data streams to achieve higher data rates, or just replace the terminal devices to upgrade a trans-Atlantic link [1]. Although optical

amplifiers provide this flexibility, and nearly limitless bandwidth, optical amplifiers also generate a wideband noise called the Amplified Spontaneous Emission (ASE) noise. ASE dominates the performance of any EDFA link and is partially removed using optical bandpass filters.

Like any electrical amplifier, EDFAs can be used as a post-amplifier, following the source, to boost the transmitted signal power, or as an in-line amplifier, mid span in a link to raise the signal levels, or as a pre-amplifier, before the receiver to improve the receiver sensitivity. For short distance applications, in-line amplifiers are seldom used because the characteristics (gain and noise) of an optical amplifier are temperature dependent. In the pre- and post-amplifier configurations, the optical amplifier can be placed in a central office or a temperature controlled environment, making the devices easy to maintain and operate. But an in-line amplifier needs a well maintained environment, and hence is more expensive to install and operate.

In this thesis we will focus on the pre-amplifier configuration and establish guidelines for the bit error ratio (BER) performance. The principal variable parameter that is at our disposal is the optical filter bandwidth, and we will examine in detail the influence of filter characteristics on performance. This thesis was supported by a research grant from Bellcore, and the experimental results were obtained by the author while employed at Bellcore during the summer of 1992. These experiments have contributed to guidelines established by Bellcore for the design of EDFA links.

Chapter 2 introduces EDFAs, discusses the working of an optical amplifier and describes the generation of the ASE noise. Chapter 3 describes the experimental setup and outlines

the data collection process using computer controlled instruments. Chapter 4 discusses the generation of beat noises in the receiver, and how they influence the BER performance. We derive a model to predict BER for a given bandwidth and other related parameters of the receiver. The predicted performance is compared with the experimental, and published results. Chapter 5 describes and predicts the optical power penalties and degradation in receiver sensitivity due to the laser center wavelength variations. The center wavelength of a laser can vary due to temperature changes, and the aging of the laser. Experimentally measured offset penalties are also presented in this chapter. Conclusions and some suggestions for further work are presented in Chapter 6.

## 2.0 INTRODUCTION TO ERBIUM DOPED FIBER AMPLIFIERS (EDFA)

Until a few years ago the most efficient way of amplifying optical signals was with repeaters. Digital repeaters convert optical signals to electrical signals, make a decision whether a 0 or 1 was received and regenerate the pulse stream. The pulse stream is used to modulate a laser and the output optical signal is injected into the fiber, effectively amplifying the optical signal. This process is expensive, and specific to a modulation scheme and data rate.

Optical amplifiers can be divided into two categories: semiconductor and fiber amplifiers. Semiconductor optical amplifiers have high coupling loss, are polarization sensitive, and possess a passband ripple. Fiber amplifiers are divided again into two categories: nonlinear and doped fiber amplifiers. Raman Scattering Emission and

Brillioun Emission use the nonlinear properties of fiber but both are inefficient and often impractical. On the other hand, doped optical fiber amplifiers provide direct amplification of optical signals, with almost no coupling loss, are polarization insensitive, efficient, and practical. An EDFA multiplies the number of signal photons, independent of the information being transmitted, hence can be used for any modulation scheme or data rate. In this thesis, we will focus only on EDFAs, and use optical amplifiers and EDFAs interchangeably.

An EDFA, as the name implies utilizes erbium doped fiber as an active medium to amplify optical signals. Erbium has an energy band diagram (Fig 2.1) such that when an electron drops from the metastable to the ground state it generates a photon in the 1520-1570 nm range [2]. Since Silica fibers have a low attenuation window at 1550 nm, erbium based amplifiers can be used to amplify communication signals. Usually a 980 nm or 1480 nm optical signal, called the pump signal, is used to excite an electron into the metastable state.

A wave division multiplexer (WDM) can be used to combine two optical signals of selected wavelengths into a given fiber. For EDFAs, a WDM is used to combine the signal photons and the pump photons into the erbium doped fiber. Depending on the pump signal, WDM may be designed to combine a 980 or 1480 nm pump signal with the 1550 nm optical signal. Hence an EDFA consists of the following three components (Fig. 2.2):

1. Doped fiber: a length of fiber (1-100 m) is doped with low concentration of erbium and sometimes co-dopants for example, $Ge_2O_3$, and $Al_2O_3$.

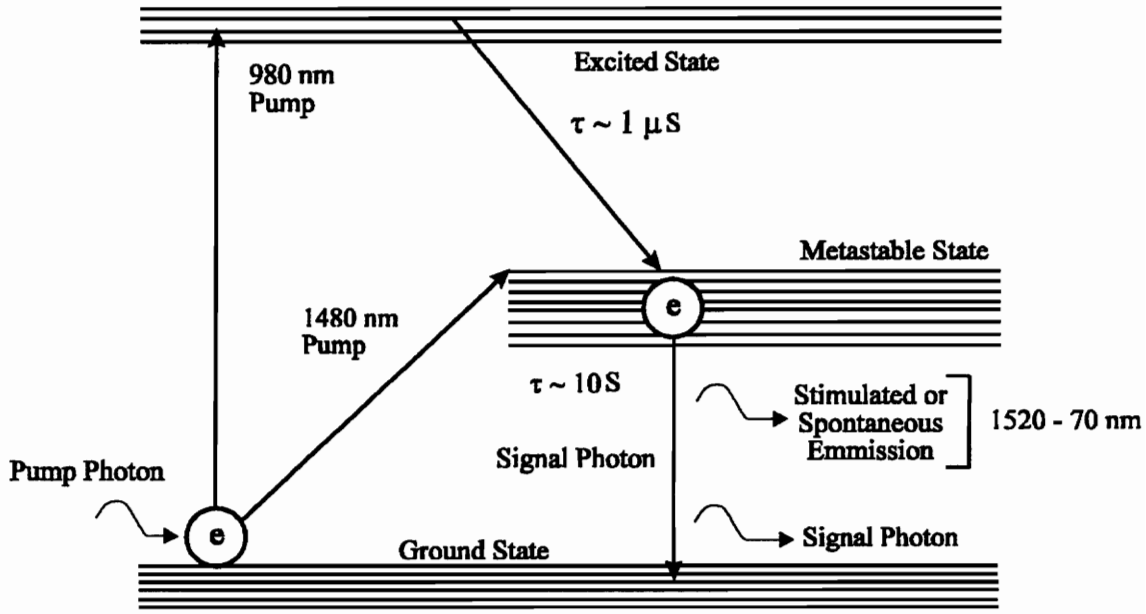


Fig. 2.1 Erbium energy band diagram [2]

2. Pump laser: a relatively high power laser (5 - 100 mW) is used to excite the erbium electrons from the ground state to higher states.
3. Wavelength division multiplexer (WDM): is used to couple both the 1550 nm information signal and the pump signal into a section of doped fiber.

The pump photons excite (pump) the ground state erbium electrons to higher states (Fig 2.1); when the electron population is flipped the atom is in a state called "Population Inversion". These electrons have short lifetimes at the higher states, hence decay to a "metastable" state quickly. Optical signals with wavelengths around 1.55 μm can stimulate the decay of an excited erbium electron to the ground state by releasing a photon with the same wavelength and phase, hence amplifying the signal. This process is called "Stimulated Emission". Due to the finite lifetimes of the electrons in the higher excited states, if an electron is not stimulated by the information signal it decays spontaneously to the ground state. This process is called "Spontaneous Emission" and results in a photon with random phase and wavelength between 1520 - 1570 nm. Just as a signal photon gets amplified, spontaneously radiated photons also get amplified hence the name amplified spontaneous emission or ASE. ASE is a wideband (1520-1570 nm) noise phenomena which impairs the BER performance, hence an optical band pass filter (BPF) is required to remove part of the ASE.

## 2.1 PUMP LASERS AND PUMPING CONFIGURATIONS

To introduce an electron into the metastable state next we look at the absorption spectrum of erbium in Fig. 2.3 [2]. The high absorption efficiency of erbium at 1550 nm, corresponds to the ability of erbium to efficiently amplify optical signals at 1550 nm. To excite the electron to the metastable state, optical signals with higher energy photons or smaller wavelengths than 1550 nm are required. Erbium can absorb photons ranging from 520-1480 nm, 980 nm pump signals have the highest absorption coefficient of the semiconductor lasers. In addition to the highest amplification efficiency, 980 nm pumps also generate the least noise and are the ideal choice for pre-amplifiers [3]. But 980 nm semiconductor lasers produce limited power, and are not as reliable as the 1480 nm lasers. Fig 2.3 shows that 1480 nm is also an efficient pumping wavelength, and InGaAs/InP lasers can provide higher optical powers, higher output saturation powers, and are more reliable. Hence, they are the more attractive choice for the post-amplifier configuration [2,3].

The pump signal can be injected into the doped fiber in either the same direction (co-propagating) or in the opposite direction (counter-propagating) as that of the information signal. In most cases performance for both configurations is comparable, but for the co-propagating configuration the remnant pump power also enters the communication system. To remove the remnant pump power, a filter or another WDM may be used, but the counter-propagating configuration (Fig. 2.2) does not require an additional component.

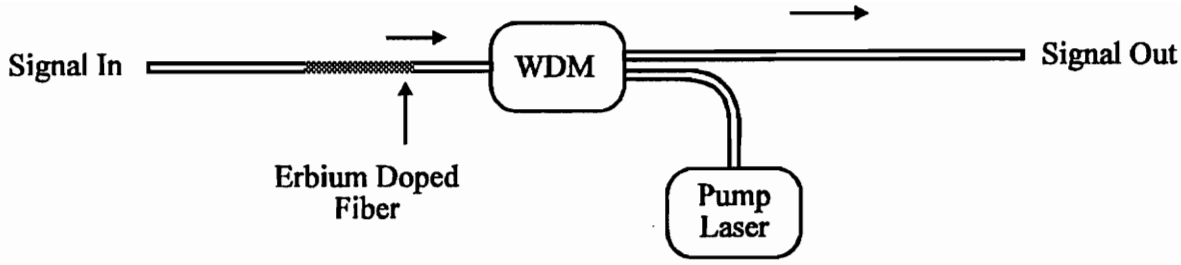


Fig. 2.2 Block diagram of an erbium doped fiber amplifier (EDFA) [3]

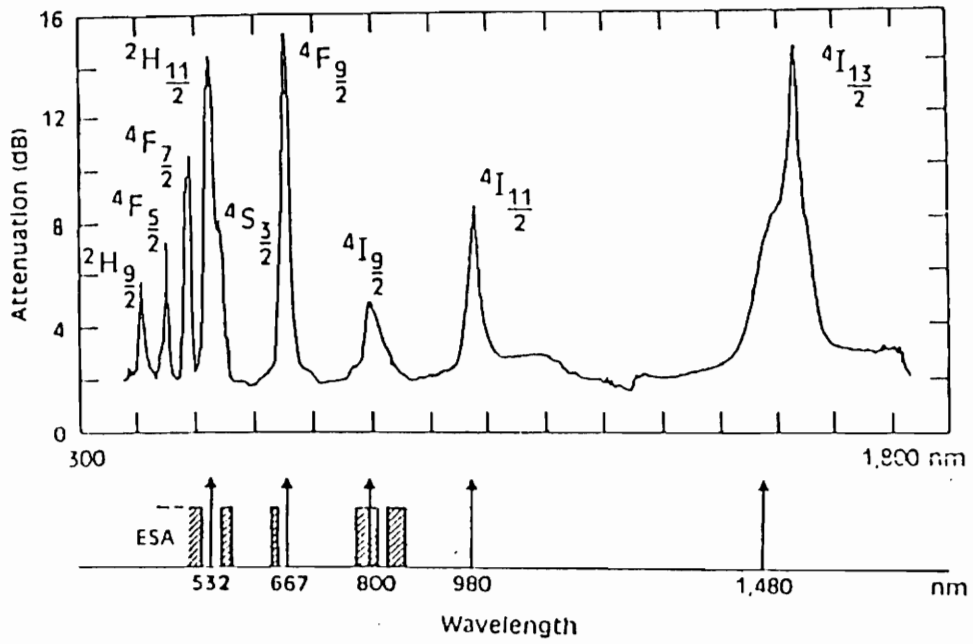


Fig. 2.3 Absorption spectrum of erbium doped fibers [2]

## 2.2 EDFA PERFORMANCE

The following paragraphs describe the effects of varying the input signal strength and the pump power on the output and the gain offered by an EDFA :

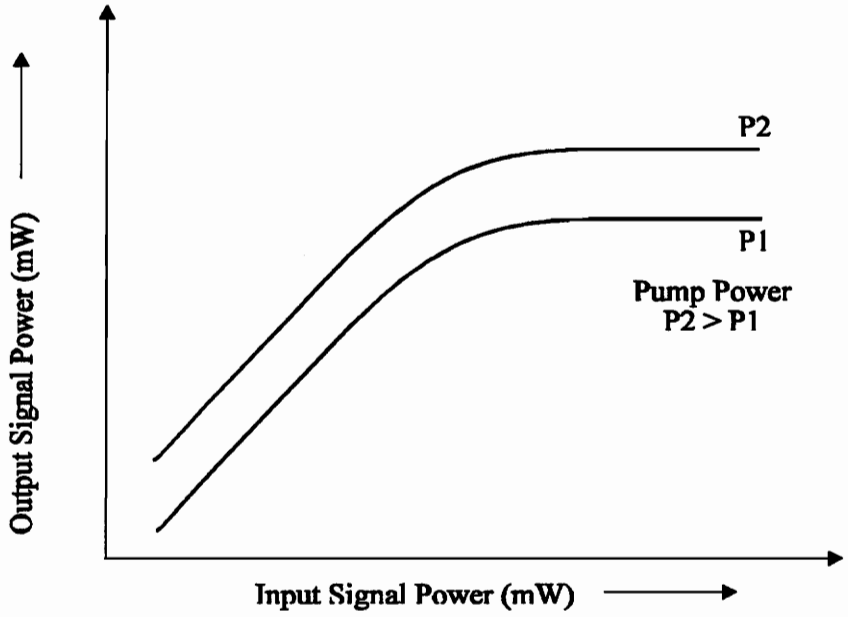


Fig. 2.4 Input vs output signal powers [3]

Output *vs.* Input Signal Strengths (Fig. 2.4): Every amplifier has a limit on the amount of output power that it can generate. At low input signal levels there are sufficient numbers of excited erbium atoms available for stimulated emissions, resulting in a linear increase of output power with input power. As the input signal power increases the ratio of excited erbium atoms to signal photon decreases leading to saturation.

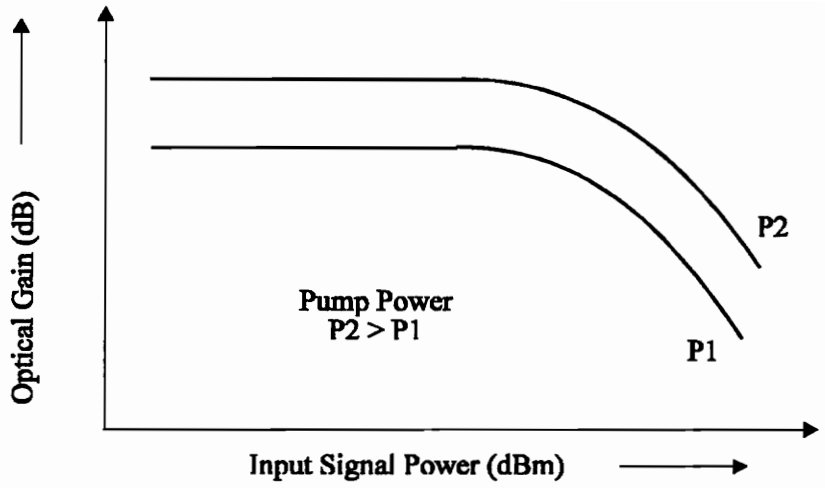


Fig. 2.5 Optical gain vs. input signal powers [3]

Optical Gain *vs.* Input Signal (Fig. 2.5): As mentioned before, for low input power the output power increases linearly with input power, hence the gain remains constant. At higher input signal powers, the optical gain starts to decrease as the amplifier enters saturation.

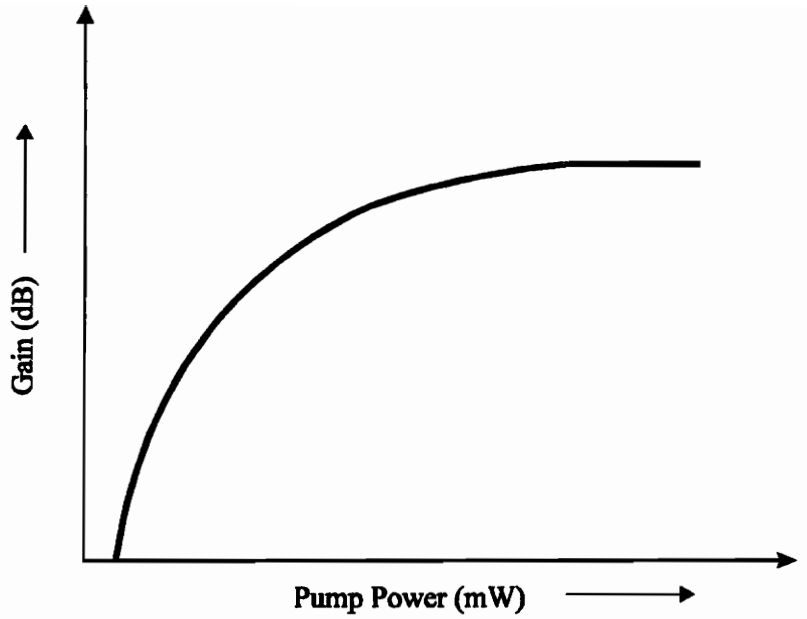


Fig. 2.6 Gain vs. pump powers [3]

Output *vs.* Pump Power (Figure 2.6): When the erbium atoms are under-pumped, they absorb all of the incoming photons, but there is no population inversion and there is no gain. There exists a pumping threshold to create a population inversion. As the pump power increases, more and more of the electrons are excited to higher states translating into higher gains. Once *all* of the erbium atoms are pumped or are waiting for the signal photon, additional pump power has no influence and the optical gain characteristic flattens and becomes independent of the pump power.

## 3.0 EXPERIMENTAL SETUP AND DATA COLLECTION

In this chapter, we describe the experimental setup (Fig. 3.1) and outline the data collection process.

To simulate a transmission link having a receiver with an optical pre-amplifier, transmission loss is introduced between the transmitter and the receiver with an optical attenuator. An ALCATEL SEL laser diode with an output power of -1 dBm and center wavelength of 1546.9 nm was used as the transmitter. When the laser diode was modulated with a 2.5 Gb/s pseudo random bit stream (PRBS), the spectral width of the laser linewidth was 0.6 nm at 20 dB below the peak power. The source was followed by an attenuator and a 1 X 2 splitter to control and monitor the power into the pre-amplifier. One of the output ports of the 1 X 2 splitter was connected to the optical amplifier, and

the second port was connected to the power meter. The output of an optical amplifier consists of two parts: (1) the amplified signal, and (2) the amplified spontaneous emission (ASE) noise. The output of the amplifier was passed through a tunable band pass filter, which consisted of two tunable 10 nm filters. By controlling the overlap between the two filters, the center wavelength and the BW of the filter was controlled. While attenuator 1 controlled the power into the EDFA, attenuator 2 controlled the signal and the ASE power allowed into the receiver. By varying attenuator 2 settings, bit error ratio (BER) vs. signal power curves were generated. The second attenuator was followed by a 1 X 2 splitter, with one of the output ports connected to the receiver, and the second port was used to monitor the optical signals. The amplified signal is superimposed on the wideband ASE, making it difficult to separate the two signals. This experimental set-up used an additional 1 X 2 splitter, and measured the total (ASE + signal) power ($P_{TOTAL}$) on one arm, and the second arm was connected to an Optical Spectrum Analyzer (OSA) to measure the peak signal power. A 0.8 dBm correction factor was added to the measured peak signal power to account for finite linewidth of the laser. The correction factor is the power lying outside the resolution bandwidth of the OSA, hence is proportional to the spectral width of the laser. This corrected measurement will be referred to as the measured signal power henceforth. The difference between the total power (measured on the power meter), and the signal power is the ASE power. The receiver used for these experiments was an ALCATEL APD with a sensitivity of -30 dBm at a BER of $10^{-9}$. An Anritsu BER meter was used to compare the output of the receiver with the expected bit stream and measure the BER.

Data was collected for four power levels into the EDFA (-29, -31, -33, and -35 dBm) and for four bandwidths (1.3, 2, 3.5, and 5 nm). For each of these sets, data was collected for

BER ranging from $10^{-4}$ to $10^{-12}$, and making this a time intensive phase of the experiments. Note that to measure a BER of $10^{-12}$ at 2.5 Gb/s requires $\approx 10^{13}$ bits or 4000 sec, which is $\approx$ 1 hour. Since the data collection process was very repetitive, a Hewlett Packard Interface Bus (HPIB) was used to control the attenuaters, the power meter, the OSA, and the Anritsu BER meter. The process of collecting data consisted of the following steps:

1. Tune the filters to the desired bandwidth, by monitoring the ASE spectrum and the signal on the OSA. This assumes that ASE noise has a constant power spectral density over the bandwidth of the filters.
2. Set attenuator 1 such that the desired power is input to the pre-amplifier.
3. Set attenuator 2, and poll the BER meter to obtain a BER reading. Similarly, the OSA and power meter were polled for the signal and the total powers measurements.
4. Repeat step 3 to collect data for BER ranging from $10^{-4}$ to $10^{-12}$.
5. Repeat steps 2 through 4 for four power levels (-29 to -33 dBm).

The data collected was written to a data file, and this data was manipulated and plotted using EXCEL. Data collected here will be referred to in later chapters as the measured or experimental performance.

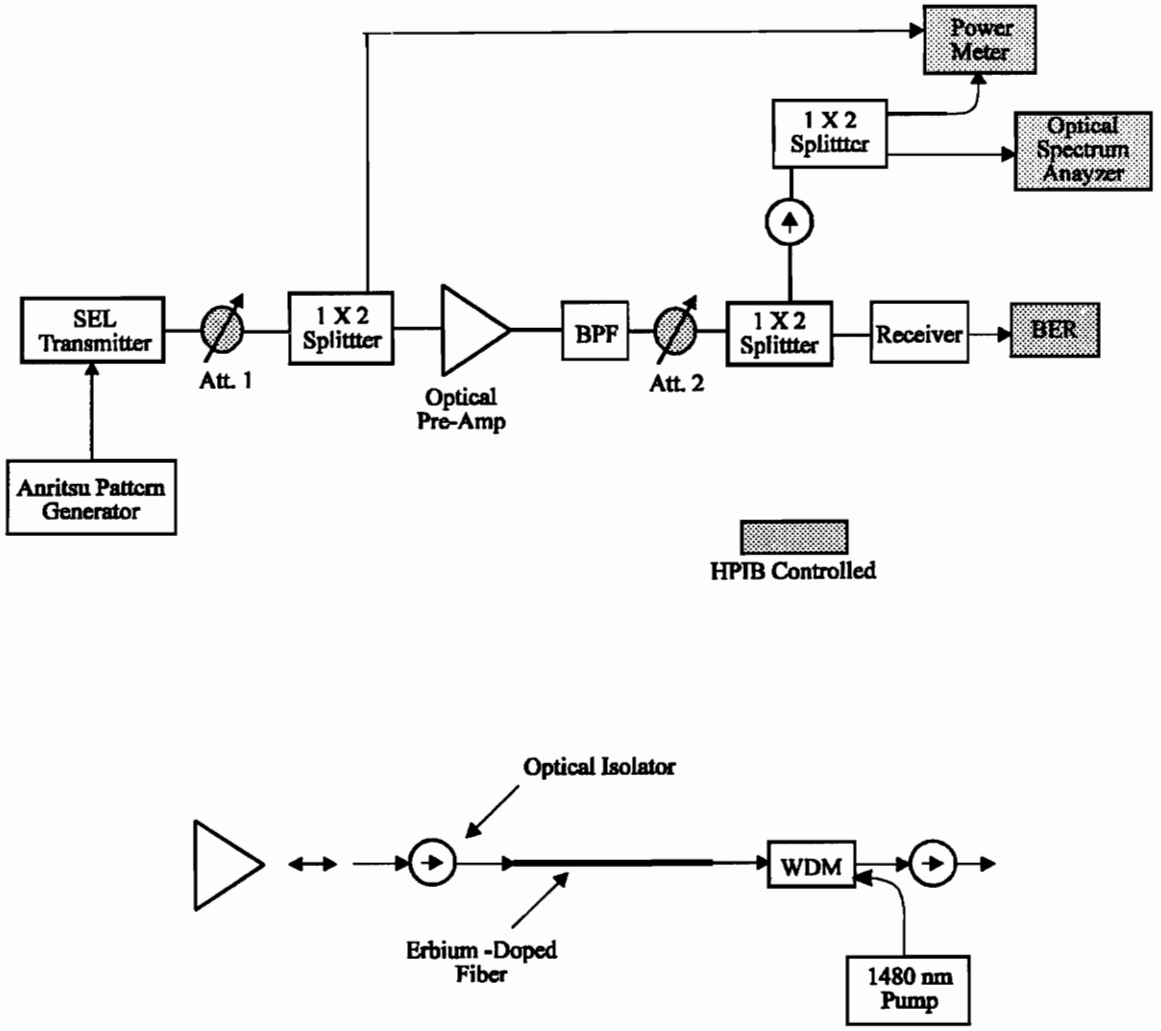


Fig. 3.1 Experimental set-up

# 4.0 DESCRIPTION OF MODEL AND DERIVATION

## 4.1 DESCRIPTION OF NOISE GENERATION

As discussed in the previous chapter, the output of the amplifier consists of the amplified signal and wideband ASE noise (Fig. 4.1). Even though the ASE noise has a low spectral density, it covers a large bandwidth (~ 40 nm), and if the entire spectral width of ASE is incident on the photodetector it will saturate the receiver, and ruin the BER performance of the system. Hence an optical BPF is required at the output of the pre-amplifier to remove part of the ASE noise and improve the performance. Intuitively it makes sense to reduce the bandwidth of the bandpass filter such that only the ASE noise within the signal bandwidth passes through, but this maybe impractical. Furthermore, it is important to understand how performance depends on the filter BW, and the characteristics of the receiver.

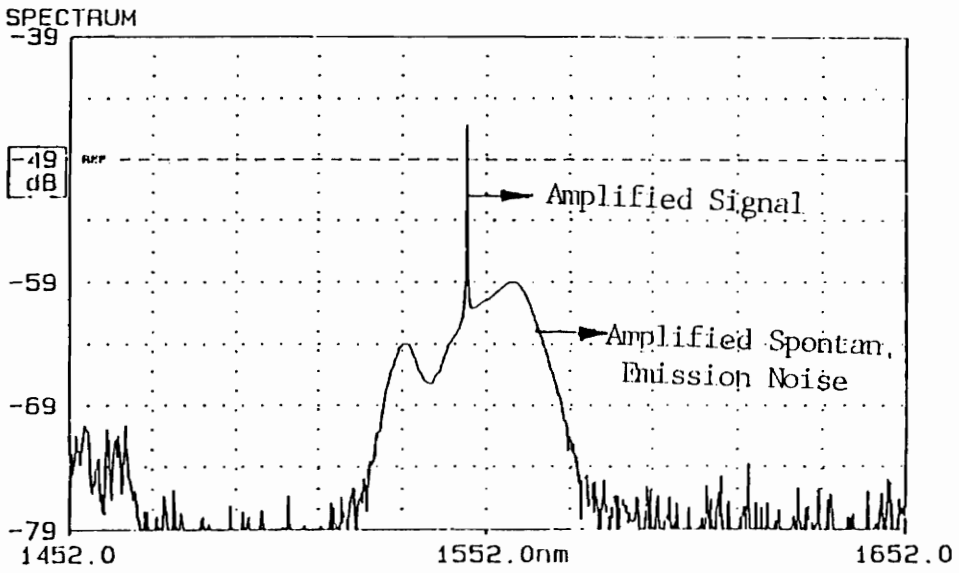


Fig 4.1 Power spectral densities of amplified signal and ASE at the output of the EDFA [3]

As mentioned earlier, there are two signals at the output of the amplifier: signal and the ASE, which are shown in Fig 4.2. Note that an optical filter was used to limit the ASE to a spectral width of 10 nm, and also note that the units for the Y-axis are arbitrary. The X-axis uses the laser's center wavelength as the origin.

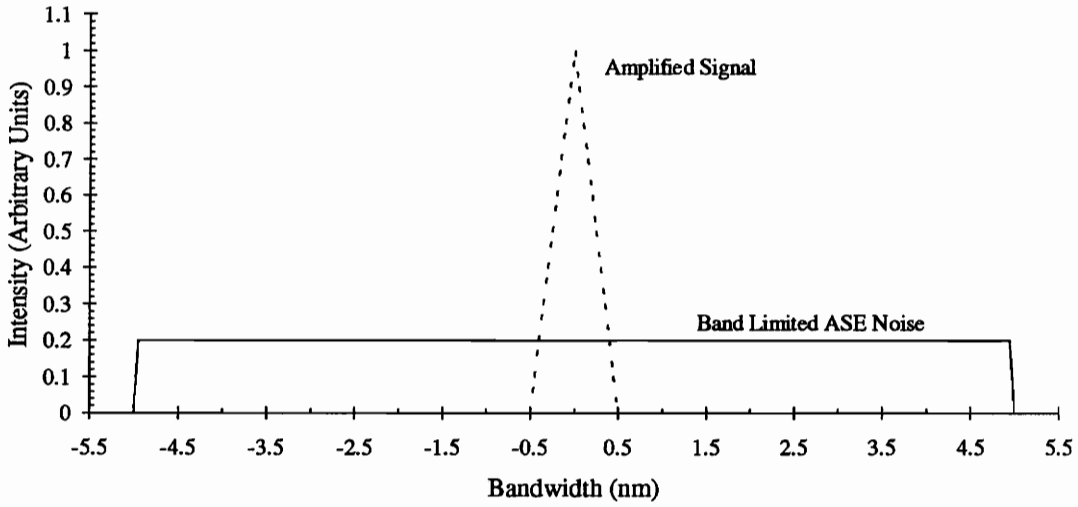


Fig. 4.2 Power spectra of the signal and the ASE noise.

The summation of these two signals is used as the input to the photodetector, and since a photodetector is a square law device, in addition to generating electrical signals for both the ASE and the information signal, it also generates a cross term. The square law action corresponds to multiplication in the time domain or convolution of the two signals in the frequency domain. Therefore, at the output of the detector we have two noise signals (1) the spontaneous-spontaneous (sp-sp) beat noise generated by the convolution of the ASE noise with itself, (2) the cross term, signal-spontaneous (sig-sp) beat noise generated by the convolution of the information signal with the ASE noise. Fig. 4.3 displays the spectra for sp-sp, and sig-sp beat noises:

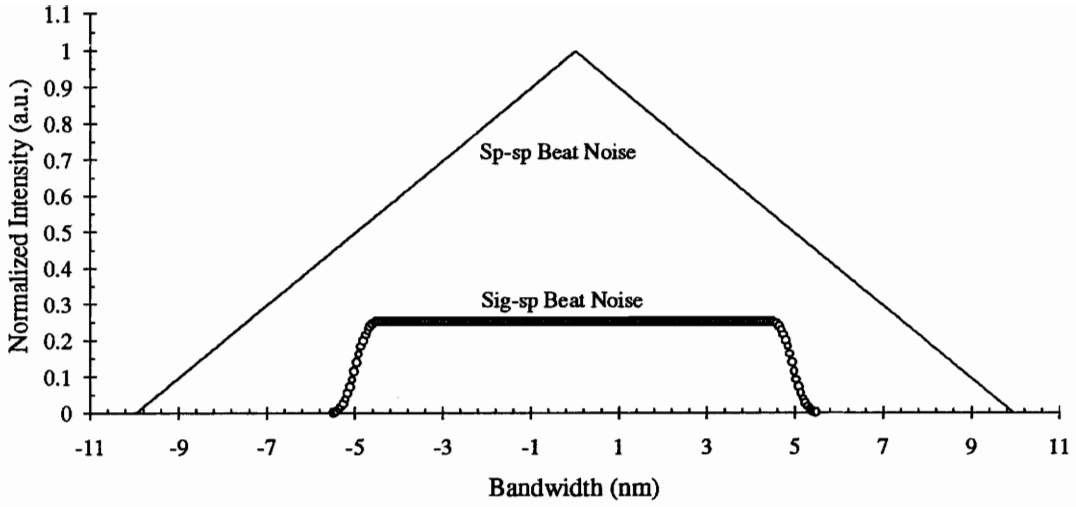


Fig 4.3 Spectrum of signal-spontaneous & spontaneous-spontaneous beat noises.

Fig. 4.3 displays the spectra of electrical noise terms at the output of photodetector. For ease of explanation and convention, the X-axis is the wavelength in nm rather than the electrical frequency. Recall that when two band limited signals are convolved, the spectral width of the output signal is the sum of the spectral widths of the two signals. This is illustrated by the spectrum of sp-sp beat noise, which has a spectral width twice that of the ASE. The spectral width of the sig-sp beat noise is the sum of the signal and the ASE spectral widths, which results in a minor increase in the spectral width of the ASE spectrum. These signals are fed to the electrical section of the receiver, which uses a lowpass filter and selects the baseband information signal and rejects everything outside the signal bandwidth. The bandwidth of the LPF depends on the data rate and the signaling used. The low pass filter rejects the bulk of the sp-sp and sig-sp beat noises, and limits the noise power allowed to pass. Hence the decision circuitry sees only a part of the power spectral densities (PSD) shown above, improving the performance. As mentioned earlier, an optical filter that selects just the signal will provide the best performance. Now consider the improvement resulting from a 5 nm filter over a 10 nm filter.

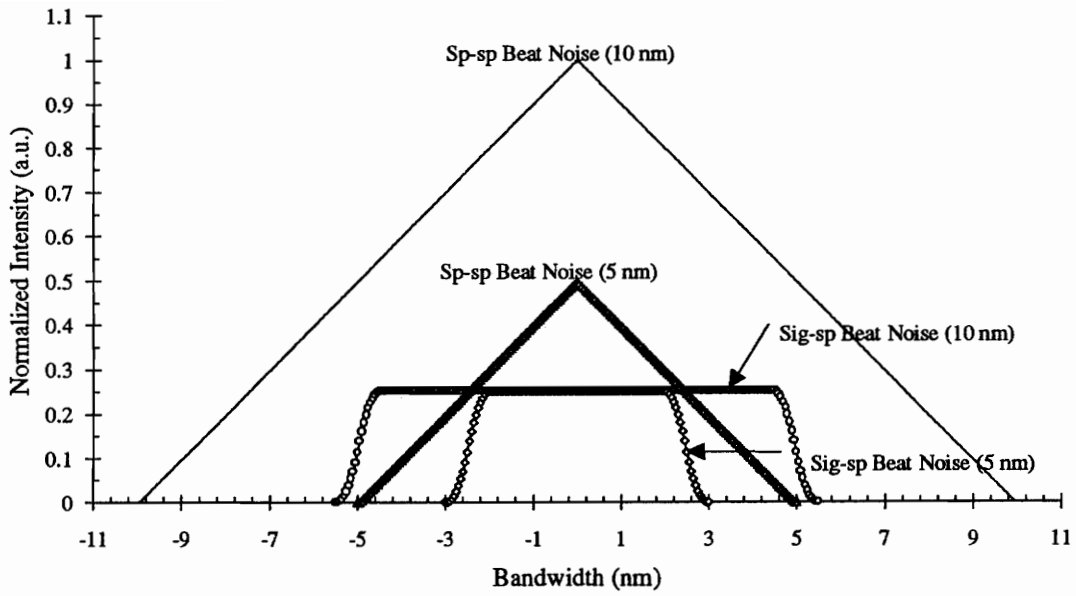


Fig. 4.4 Power spectral densities of beat noises for 5 & 10 nm filters.

The same normalizing coefficients were used as in Fig. 4.3 to normalize both the 5 and 10 nm data. For sp-sp beat noise, its clear that the magnitude of the PSD for the 5 nm case should be half that for the 10 nm bandwidth case. Furthermore, the spectral width of the sp-sp beat noise for the 10 nm filter should be 20 nm while that for the 5 nm filter should be 10 nm. Note that the magnitude of the PSD for sig-sp beat noises are equal for both 5 and 10 nm filters, and the spectral width for the 10 nm filter is larger than the 5 nm filter. Let's examine the effect of the electrical low pass filter. The sig-sp beat noise captured for the 5 nm and 10 nm case is exactly the same. However, the sp-sp beat noise captured by the electrical filter, as displayed in Fig 4.4 is a function of the optical bandwidth. The 10 nm filter presents more sp-sp beat noise than the 5 nm filter when passed through the electrical LPF. Hence the sig-sp beat noise seen by the decision circuitry is not a function of the optical bandwidth, while the sp-sp beat noise, which dictates the performance, is a strong function of the optical bandwidth.

Summarizing, ASE has a spectral width of ~ 40 nm, and if all of the ASE impinges on the photodetector, the receiver will saturate and the performance will degrade. An optical bandpass filter can alleviate this problem, by removing a portion of the ASE noise and improving the performance. The optical bandwidth only impacts the sp-sp beat noise, which controls, or dictates the performance. This material has been described well by N. Olsson in "Lightwave Systems with Optical Amplifiers", *Journal of Lightwave Technology* of July 1989 [4]. Tonguz and Kazovsky have also published a paper describing the noise phenomena in "Theory of Direct Detection Lightwave Receivers Using Optical Amplifiers" *Journal of Lightwave Technology* of February 1991 [5].

## 4.2 DERIVATION OF MODEL TO PREDICT BER

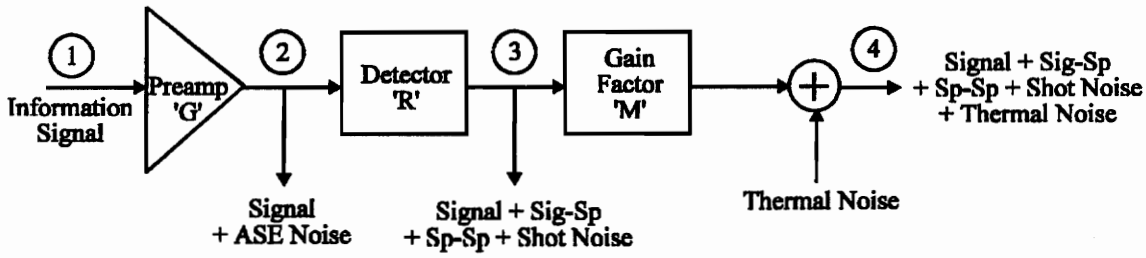


Fig. 4.5 Block diagram of an EDF pre-amplifier followed by an APD receiver

This model breaks the receiver down into individual blocks (Fig. 4.5), and calculates the signal and noise currents at various steps in the receiver. The APD receiver consists primarily of two stages: first is a photodetector which converts the optical signal to an

electrical signal, and has a responsivity 'R'. Responsivity is the efficiency of a detector, and is given by:

$$R = \frac{I_{ph}}{P_s}\left[\frac{A}{W}\right] \tag{4.1}$$

Where $I_{ph}$ is the primary photocurrent generated from the incident optical power $P_S$. The second stage of an APD receiver is the gain or the multiplication factor 'M'. All the currents passed through this stage experience a gain of M.

At stage 1 in Fig. 4.5, a weak information signal is received at the input to the receiver, where a receiver comprises of an optical pre-amplifier followed by an APD receiver. For an ideal On-Off Keying (OOK) digital system when a '1' is received the carrier is present, and in the off state there is no signal. This can be written as:

$$S = \begin{cases} \frac{A}{\sqrt{G}} Cos(2\pi f_c t) & : 1 \\ 0 & : 0 \end{cases} \tag{4.2}$$

*A is the amplitude referred to stage* 2; $f_c$ *is the* optical *carrier frequency*

$$Let \quad 2\pi f_c = \omega_c$$

At stage 2, the output of the amplifier consists of the amplified signal and ASE noise. ASE is a Gaussian random process. The ASE noise is divided into in-phase and out of phase components relative to the signal. The signal at stage 2 can be expressed as:

$$S = \begin{cases} (A+x)Cos(\omega_c t) + ySin(\omega_c t) & : \quad 1 \\ xCos(\omega_c t) + ySin(\omega_c t) & : \quad 0 \end{cases} \tag{4.3}$$

*x and y are in− and out of phase components of ASE*

Part of the ASE is removed using the band pass filter (not shown), and the output is fed to the APD. The detector squares the optical information signal and the ASE noise. The square law action generates the signal, the signal-spontaneous (sig-sp) and the spontaneous-spontaneous (sp-sp) beat noise currents. In addition, the photodetector adds a Poisson distributed random noise, called the shot noise. Here only the signal shot noise is considered, and the shot noise generated due to the ASE is ignored. To express the signal at the output of the detector, we must account for the low pass filter. Low pass filtering is equivalent to weighing the frequency components of the input signal with the filter's response, but this technique is very cumbersome. Instead, in the time domain the filter can be modeled as a discrete time integrator (with a small error) by the following impulse response [5]:

$$h_{LPF}(t) = \sum_{i=1}^{BT} \delta\left(t - \frac{i}{B}\right) \tag{4.4}$$

Where B represents the optical bandwidth of the receiver in Hertz, and T is the bit period (1/Rb, Rb is the bit rate). This impulse response corresponds to averaging BT independent samples of the current at the output of the photodetector every 1/B seconds. Therefore, the output of the post detection filtering including ASE is given by [7]:

$$S = \begin{cases} \frac{1}{2m}\sum_{i=1}^{m}\left[(A+x_i)^2 + y_i^2\right] + i_{sh} & : 1 \\ \frac{1}{2m}\sum_{i=1}^{m}\left[x_i^2 + y_i^2\right] & : 0 \end{cases} \qquad m = BT, \text{ the bandwidth time period product;} \qquad (4.5)$$

$i_{sh}$ *is the signal shot noise current*

The second stage of the APD receiver (the gain or multiplier), amplifies all the currents being passed through, and the currents are multiplied by a uniform factor 'M'. The electrical part of the receiver adds thermal noise, which is a function of the electrical properties (amplifier and filters) of the receiver and independent of the optical signal strengths. The output of the receiver at stage 4 in Fig. 4.5, is fed to the decision circuitry and is expressed as:

$$S = \begin{cases} \frac{1}{2m}\sum_{i=1}^{m}\left[(A+x_i)^2 + y_i^2\right] + i_{sh} + i_{th} & : 1 \\ \frac{1}{2m}\sum_{i=1}^{m}\left[x_i^2 + y_i^2\right] + i_{th} & : 0 \end{cases} \qquad \text{where } i_{th} \text{ is the thermal noise current} \qquad (4.6)$$

The decision circuitry sees the composite signals in Equation 4.6, and decides whether a 1 or 0 was received. The performance of a digital communication system is expressed in terms of bit error ratio (BER), which is a function of the signal and the noise currents. Using the Gaussian approximation, the BER can be expressed as:

$$BER = Q(\kappa)$$

$$where\ \kappa = \frac{\mu_1 - \mu_0}{\sigma_1 - \sigma_0} \tag{4.7}$$

$\mu_1 = mean\ of\ the\ current\ in\ the\ on-state;\ \mu_0 = mean\ of\ the\ current\ in\ the\ off-state$

$\sigma_1^2 = variance\ in\ the\ on-state;\ \sigma_0^2 = variance\ in\ the\ off-state$

Kappa ($\kappa$) is an effective SNR, and is a measure of the performance of the system. To set up the expression for kappa, the information and noise currents must be referred to a fixed point in the receiver (Fig. 4.5). Since the measured quantities are optical powers, it makes sense to use optical powers and refer the currents to the output of the pre-amplifier or the input to the photodetector at stage 2 in Fig. 4.5. This involves expressing the currents in terms of the measured optical powers, by using the responsivity 'R', and the gain factor 'M' of the receiver. Some assumptions can be made about the signals to simplify the expression for kappa. For example, $i_{th}$ has a Gaussian distribution with a mean of zero, and $i_{sh}$ also has a mean of zero hence neither appear in the numerator of Equation 4.7. It is also assumed that the samples of $x_i$ and $y_i$ (in- and out-of phase components of ASE) are independent identically distributed Gaussian variables. This also implies that the mean of sig-sp beat noise is zero. By combining all these assumptions the mean of currents in the on- and off-stage can be calculated [6,7]:

$$\mu_0 = \overline{S_0} = \sigma^2_{ASE} = P_{ASE}$$

$$where\ \overline{x_i^2} = \overline{y_i^2} = \sigma^2_{ASE} = P_{ASE}$$

$$\mu_1 = \overline{S_1} = \overline{\frac{A^2}{2} + x_i^2 + Ax_i + i_{sh} + i_{th}} = 2P_s + \sigma^2_{ASE} = 2P_s + P_{ASE} \qquad (4.8)$$

$$where\ \frac{A^2}{2} = 2P_S;\ P_S = Average\ or\ measured\ signal\ power$$

$$\therefore\ \mu_1 - \mu_0 = 2P_S$$

Next we calculate the variance of the currents or the noise powers in the on- and off-stages, and set up the denominator of Equation 4.7 [6]:

$$\sigma_1^2 = \frac{A^2\sigma^2_{ASE}}{m} + \frac{\sigma^4_{ASE}}{m} + \sigma^2_{th} + \sigma^2_{sh};\quad \sigma_0^2 = \frac{\sigma^4_{ASE}}{m} + \sigma^2_{th}$$

$$\sigma^2_{th} \equiv Thermal\ Noise = \frac{4kTB_e}{M^2R^2Z_e};\ \sigma^2_{sh} \equiv Sig.\ Shot\ Noise = \frac{2qFB_eM^2I_{ph}}{M^2R^2} = \frac{4qFB_eRP_s}{R^2}$$

$$\frac{A^2\sigma^2_{ASE}}{m} \equiv Signal - spontaneous\ beat\ noise \qquad (4.9)$$

$$\frac{\sigma^4_{ASE}}{m} \equiv Spontaneous - spontaneous\ beat\ noise$$

$$\sigma_1 + \sigma_0 = \sqrt{\frac{4P_s\sigma^2_{ASE}}{m} + \frac{\sigma^4_{ASE}}{m} + \frac{4kTB_e}{M^2R^2Z_e} + \frac{4qFB_eP_s}{R}} + \sqrt{\frac{\sigma^4_{ASE}}{m} + \frac{4qFB_eP_s}{R}}$$

In the above equation, $B_e$ is the electrical bandwidth of the receiver, F is the excess noise factor of the APD, and $Z_e$ is the noise impedance of the electrical part of the receiver. The expressions for $\sigma^2_{sh}$ and $\sigma^2_{th}$ were determined as follows. To refer the thermal noise power to the input of the multiplier of the APD, it is normalized using $M^2$ (Fig. 4.5). The multiplication factor works on the current, and since power is proportional to current

square, $M^2$ is used as the normalizing coefficient. Similarly, the next step involves referring the thermal noise to the input of the detector, which uses $R^2$ as the normalizing coefficient [6]. The shot noise is also normalized using the same coefficients. Now Equation 4.7 can be expressed in terms of the optical powers, by combining both Equations 4.8, and Equation 4.9:

$$\kappa = \frac{2P_s}{\sqrt{\frac{P_{ASE}}{m}(4P_s + P_{ASE}) + \frac{4kTB_e}{Z_e M^2 R^2} + \frac{4qFB_e}{R}P_s} + \sqrt{\frac{P_{ASE}^2}{m} + \frac{4kTB_e}{Z_e M^2 R^2}}} \tag{4.10}$$

Using Equation 4.10, kappa can be calculated, or performance predicted for a given pre-amplifier receiver.

Although the gain of the optical amplifier (G) does not appear explicitly in Equation 4.10, it does affect the performance. The ASE noise power ($P_{ASE}$) is given by:

$$P_{ASE} = 2n_{sp}(G-1)hfB \tag{4.11}$$

where $n_{sp}$ is the spontaneous emission factor of the amplifier, hf is the energy in the signal photon, and B is the optical bandwidth of the receiver. The factor of '2' accounts for the equal noise power in the two polarizations of the ASE. The ASE noise power is linearly proportional to the gain of the optical amplifier. Similarly, the signal power ($P_S$) at the input of the APD is also linearly proportional to the gain of the amplifier. Since thermal noise (Equation 4.9) is independent of the optical signals, under high gain conditions the thermal noise will be negligible. Furthermore, sp-sp and sig-sp beat noises are proportional to $G^2$, whereas the signal shot noise term, is proportional to G. Thus, if G is sufficiently large (greater than about 20 dB), both the numerator and denominator of

Equation 4.10 are proportional to G and the overall performance is independent of the gain of the amplifier and the receiver properties. The BER performance is dependent on the properties of the optical amplifier such as the optical bandwidth (B), $n_{sp}$, and saturation power of the optical amplifier. The APD receiver behaves like a cascade of amplifiers, where the first stage is the optical preamplifier. For a cascade, when the gain of first stage is high, the performance is a strong function of the noise properties of the first stage, and independent of the following stages. From Equation 4.10 it is clear that under the high gain scenario, the performance is independent of the APD, and is only a function of the EDFA [7,8].

### 4.2.1 BASELINE CHARACTERIZATION

To characterize the APD receiver, the baseline (without the optical amplifier) performance was measured and signal power vs. BER curve was generated (Fig. 4.6). For the baseline receiver $P_{ASE} = 0$, and Equation 4.10 is modified to give the following expression for kappa:

$$\kappa = \frac{P_s}{\sqrt{\frac{kTB}{Z_e M^2 R^2} + \frac{qFB}{R} P_s} + \sqrt{\frac{kTB}{Z_e M^2 R^2}}} \tag{4.12}$$

$$Let\ a = \frac{qFB}{R}; \qquad b = \frac{kTB}{Z_e M^2 R^2};$$

$$\therefore\ \kappa = \frac{P_s}{\sqrt{b + aP_s} + \sqrt{b}}$$

In Equation 4.12, $P_S$ and $\kappa$ are known from baseline measurements but 'a' and 'b' depend on the APD. For an APD receiver F and M are signal dependent, therefore 'a' and 'b' cannot be calculated accurately. For a good receiver, performance is determined more by 'a', than by 'b' because of the presence of $M^2$ in the denominator of 'b'. Consequently, we will use typical system parameters to calculate 'b' and then use the baseline measurements to determine 'a':

$$k = 1.381 \times 10^{-23} \ \frac{J}{K}; \ T = 290 \ K; \ B = 1.4 \times 2.48832 \times 10^{9} \ \ Hz \text{ (NRZ Signaling)}; \quad (4.13)$$

$$R = 0.7 \ \frac{A}{W}; \ M = 5; \ Z_e = 1000\Omega$$

$$\therefore \ b = \frac{kTB}{Z_e M^2 R^2} = 1.14 \times 10^{-15} \ \ W^2$$

For NRZ signaling the electrical bandwidth required is 1.4 times the data rate. Using the estimated value of 'b' and Equation 4.12, the value of 'a' can be calculated for each of the data points for the baseline receiver. This is illustrated in Table 4.1:

Table 1: Baseline measured performance

| **Measured Data For the Baseline Reciever** | | | | | |
|---|---|---|---|---|---|
| | | | | | |
| *b = 1.1389e-15* | | | | | |
| | | | | | |
| **Ps (dBm)** | **Ps (Watts)** | **Log(BER)** | **Kappa** | **a** | **% variation** |
| | | | | | |
| -33.25 | 4.73E-07 | -3.921 | 3.7 | 1.632E-08 | -0.12 |
| -33 | 5.01E-07 | -4.155 | 3.9 | 1.564E-08 | 4.02 |
| -32.75 | 5.31E-07 | -4.409 | 4 | 1.631E-08 | -0.04 |
| -32.25 | 5.96E-07 | -5.000 | 4.3 | 1.652E-08 | -1.34 |
| -31.75 | 6.68E-07 | -5.638 | 4.6 | 1.691E-08 | -3.76 |
| -31 | 7.94E-07 | -6.854 | 5.2 | 1.640E-08 | -0.59 |
| -30.5 | 8.91E-07 | -7.796 | 5.6 | 1.637E-08 | -0.41 |
| -30.25 | 9.44E-07 | -8.319 | 5.75 | 1.682E-08 | -3.16 |
| -30 | 1.00E-06 | -8.921 | 6 | 1.653E-08 | -1.40 |
| -29.75 | 1.06E-06 | -9.509 | 6.2 | 1.667E-08 | -2.27 |
| -29.5 | 1.12E-06 | -10.260 | 6.5 | 1.617E-08 | 0.78 |
| -29.25 | 1.19E-06 | -11.222 | 6.8 | 1.578E-08 | 3.21 |
| -28.75 | 1.33E-06 | -12.921 | 7.35 | 1.550E-08 | 4.90 |
| | | | | | |
| | | | ***Average a =*** | ***1.630E-08*** | |

The first column contains the signal powers in dBm, which are converted to Watts in the second column. Using the measured BER, and Q function tables the kappa is calculated, and the corresponding values of 'a' are calculated using the following equation:

$$a = \frac{\left(\frac{P_s}{\kappa} - \sqrt{b}\right)^2 - b}{P_s} \tag{4.14}$$

The last column is the percentage variation in 'a' from the calculated average value. Note that the calculated values of 'a' are nearly constant ($1.63 \times 10^{-8} \pm 4.9\%$). From the calculated value of 'a', the excess noise factor 'F' can be extracted to fully characterize the APD and also check the parameters of the receiver. From Equation 4.12:

$$F = \frac{aR}{qB} = 20.34 \tag{4.15}$$

The noise factor around 20 is on the high side for a state of the art receiver, but is not unreasonable.

The average value of 'a' can be used to calculate the baseline performance to compare with the measured performance. The comparison graph is shown in Fig. 4.6. Note that the measured and the calculated performances are very close, indicating that the values approximated to calculate 'b' were reasonable. The model can accurately characterize the noise, and the performance of the APD receiver. The close match in Fig. 4.6 also validates the baseline receiver model.

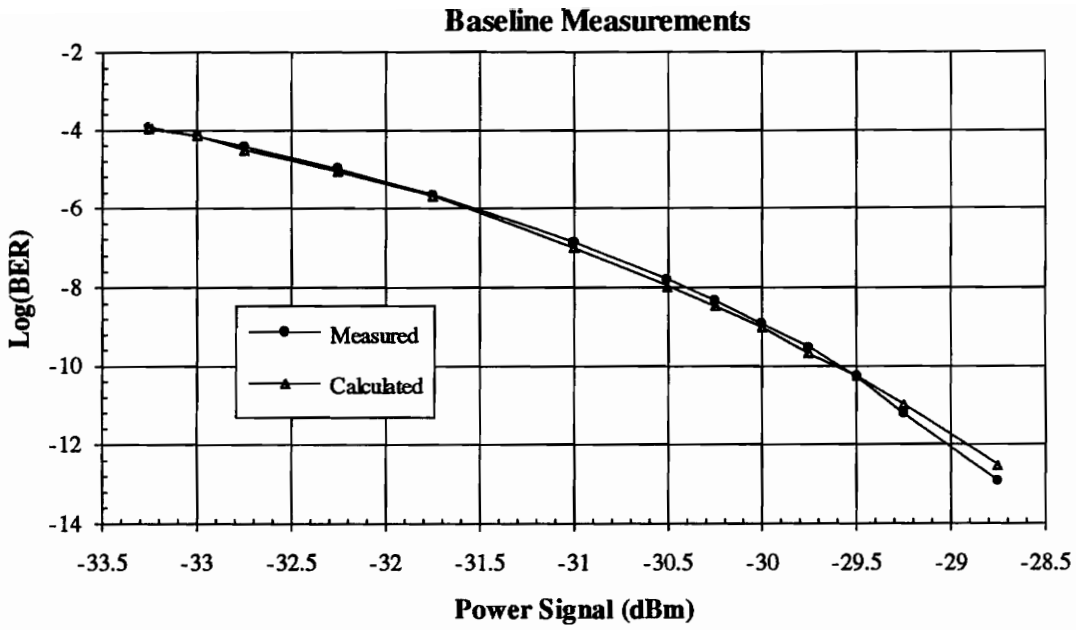


Fig. 4.6 Comparison between baseline measured and calculated performances

## 4.3 DISCUSSION OF MODEL

The model in Equation 4.10, can be rewritten as:

$$\kappa = \frac{2P_s\sqrt{m}}{\sqrt{P_{ASE}(P_{ASE}+4P_S)+4m(b+aP_s)}+\sqrt{P_{ASE}^2+4bm}} \tag{4.16}$$

This model can be used to predict the performance of a pre-amplifier APD receiver for a given optical bandwidth, and signal level. This section compares the performance predicted by this model, with the measured performance from the experiments, for all the measured signal powers and all the bandwidths. Later in this section we compare this model, with a published model, and discuss the differences. Lastly we will discuss possible sources of differences between the measured and calculated performances.

### 4.3.1 COMPARISON WITH MEASURED RESULTS

Let's start by comparing the experimental results with the predicted performances. Here kappa is used as a normalized measure of performance. As mentioned earlier BER=Q(κ), where kappa of 6 corresponds to a BER of $10^{-9}$, and kappa of 7 corresponds to BER of $10^{-12}$. The Q function is a very strong function of the argument, and rolls off steeply as shown in Appendix 1. The following graphs, plot kappa on the Y-axis, and the signal power as measured on the OSA on the X-axis. The graphs display results for various signal powers and optical bandwidths.

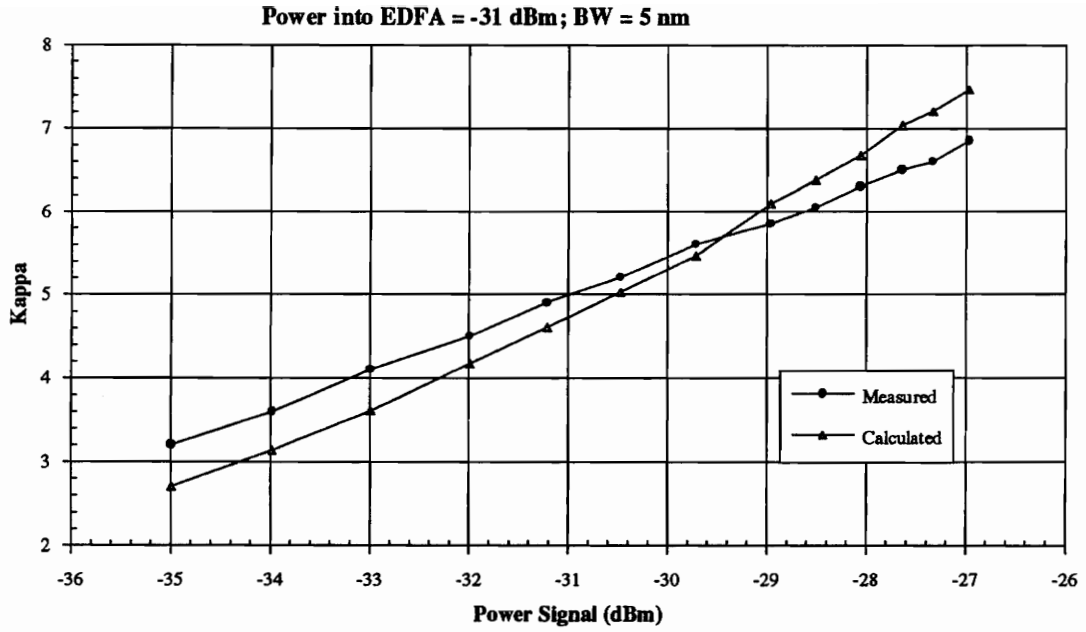


Fig. 4.7 Comparison between the measured and the calculated performances

Fig. 4.7 displays the performance for -31 dBm into the EDFA, and an optical BW of 5 nm. The match between the measured and calculated results is good. Note that for low signal powers the measured curve performs better (has a higher kappa, translating into a lower BER) but for higher signal levels, the calculated curve performs better. This may be due to the saturation of the electrical part of the receiver for high input powers. In addition to the signal power, ASE noise is also incident on the photodetector which is of the same order of magnitude as the signal power. Hence the total (signal + ASE) power might lead to the saturation of the receiver and degrade the performance of the system at higher signal levels. Overall the measured and the calculated curves track reasonably closely.

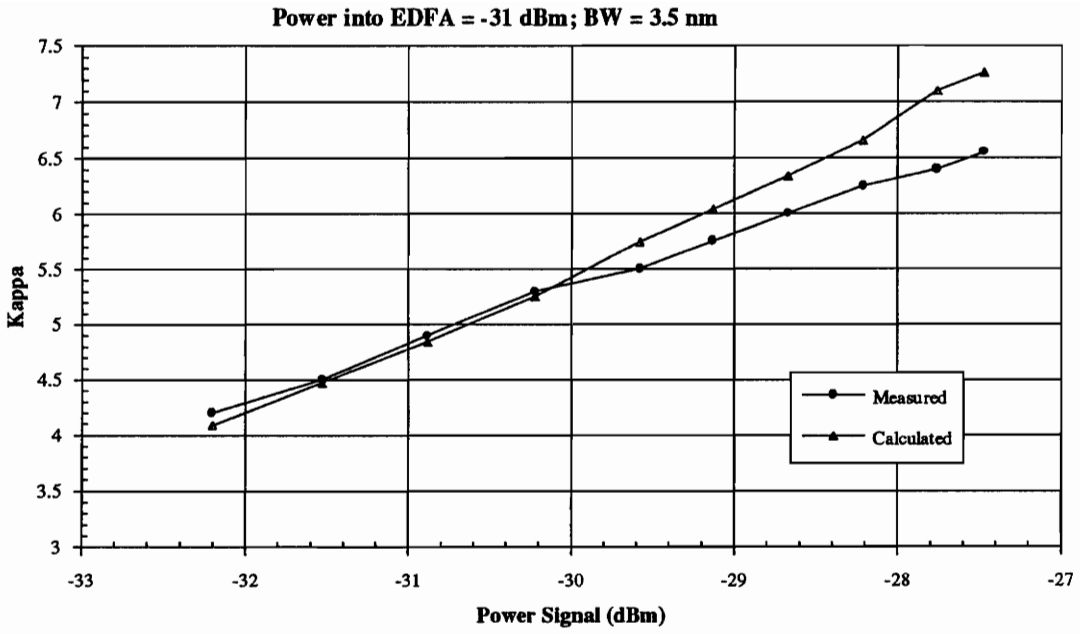


Fig. 4.8 Comparison between the measured and the calculated performances

Fig. 4.8 displays the comparison between the measured and the calculated kappas for -31 dBm into the EDFA, and an optical BW of 3.5 nm. Note that "calculated results" are calculated from the model using measured values of $P_S$ and $P_{ASE}$. Also note that $P_{ASE}$ is measured by subtracting $P_S$ from $P_{TOTAL}$. An error in $P_{TOTAL}$ will only manifest itself in the calculated results. Furthermore, as mentioned earlier, the bandwidth of the filters were calibrated assuming that the ASE has a constant PSD. Therefore, discrepancies between the measured and calculated results could well be due to the uncertainties in the measurements.

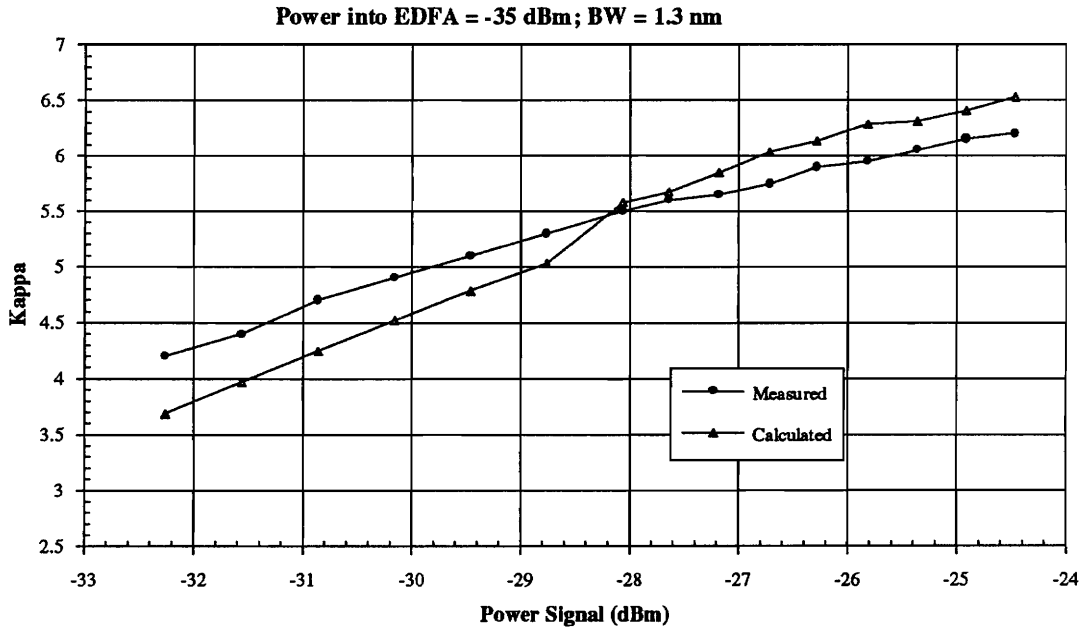


Fig. 4.9 Comparison between the measured and the calculated performances

Fig. 4.9 compares the measured and calculated performance with -35 dBm input to the EDFA, and an optical BW of 1.3 nm. The discrepancy at the lower signal levels does not translate into significant error in BER due to the gradual roll-off of the Q function at the lower values of kappa (Appendix 1). Similar to the previous cases, the measured performance at higher signal levels is poorer than the calculated results. As noted before, this may be a result of saturation in the electrical portion of the receiver. Another possible reason could be a signal dependent noise source; for example, Relative Intensity Noise (RIN), which degrades the performance (noticeably) at higher signal levels.

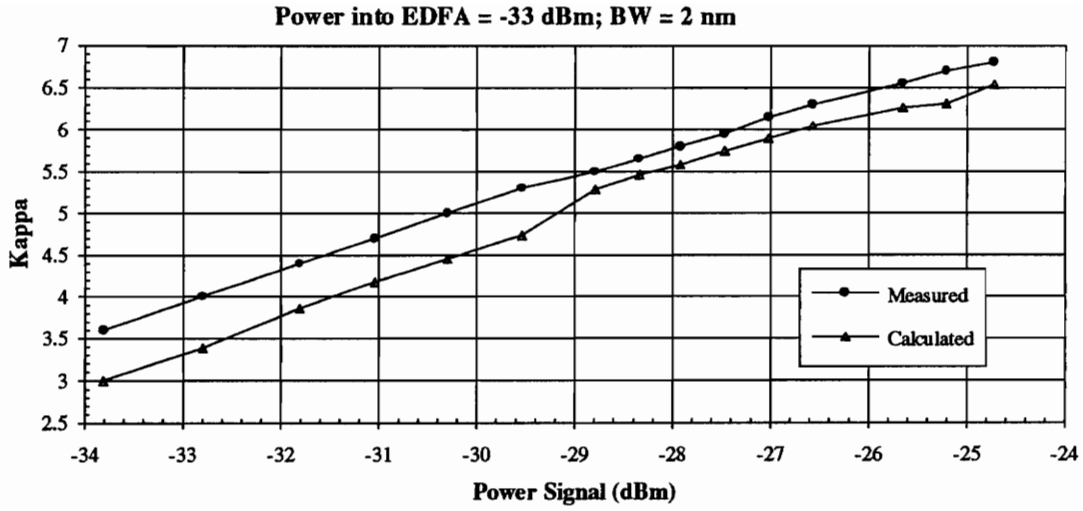


Fig. 4.10 Comparison between the measured and the calculated performances

Fig. 4.10 displays the calculated and measured results for -33 dBm signal power input to the EDFA and an optical BW of 2 nm. Note here that the measured and the calculated results do not intersect unlike the other graphs. Also note that there is a jump in the calculated performance at -29.5 dBm, whereas the measured curve takes a downturn in kappa at the very same data point. This may be associated with a small error in the power meter measurement which reduces the $P_{ASE}$ effectively giving the calculated performance a jump. Nevertheless, the curves track reasonably closely and the error between the measured and the calculated performance curves is small.

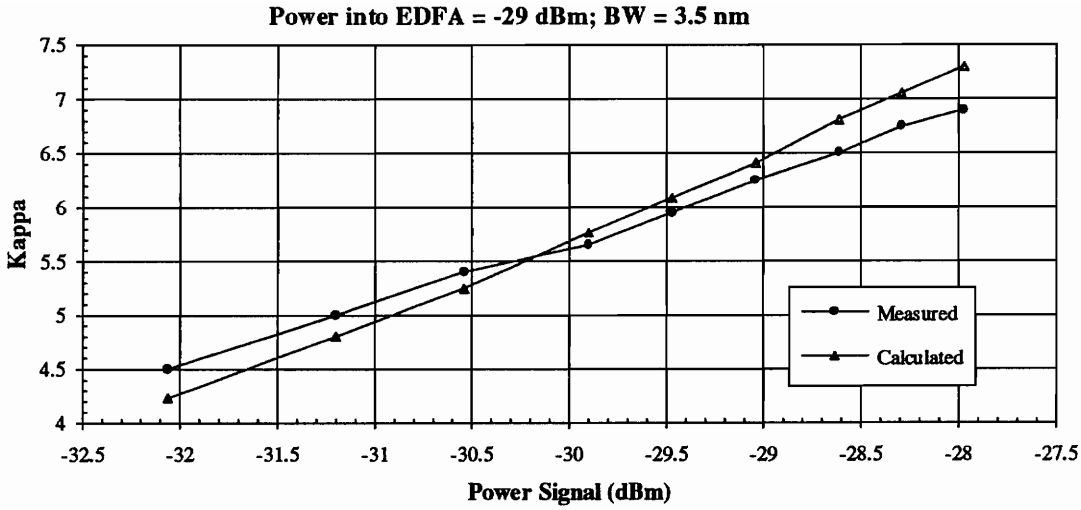


Fig. 4.11 Comparison between the measured and the calculated performances

This last graph compares the performances for -29 dBm signal power into the EDFA, and an optical BW of 3.5 nm. The performance curves track closely and the match is good. A similar intersection is seen as an Fig. 4.8 and 4.9.

Summarizing the previous five graphs, the model presented here does a good job in predicting and tracking the performance for an EDF pre-amplified APD receiver for various signal levels and optical bandwidths. We note that the discrepancies may be due to saturation effects which are device dependent and cannot be modeled for any APD. The errors may also be caused by signal dependent noise sources, or errors in signal or bandwidth measurements. In conclusion, there is general agreement between the measured and calculated results.

### 4.3.2 COMPARISON WITH PUBLISHED RESULTS

There exist general papers about the state of the art achieved performances, and other papers describing the noise phenomena, but not very many papers that describe, and predict the noise phenomena and performance. One such paper was published by Ruhl and Ayre, "Explicit Expressions for the Receiver Sensitivity and System Penalties of Optically Preamplified Direct Detection Systems" *Photonics Technology Letters* of March '93 [8]. This paper presented an all theoretical analysis of an EDF pre-amplifier system with an APD receiver, which comes close to the work presented here. Next we compare the model presented here with these published results.

The authors of [8] derived a model, and presented performance curves for a theoretical system and set of parameters. Fig 4.12 displays one such curve, where the authors have plotted receiver sensitivity in dBm vs. optical BW for a BER of $10^{-12}$. This figure contains data for 622 Mb/s and 2.5 Gb/s, with a laser centered at 1540 nm. To compare the two models, we use the parameters in [8] to generate the baseline characterization parameters 'a' and 'b'. The calculated baseline parameters are then substituted into Equation 4.16 to calculate value of kappa for the optical BW of 2 nm, with 2.5 Gb/s and extinction ratio r = 0.1. Fig. 4.13 displays the block diagram used in [8]:

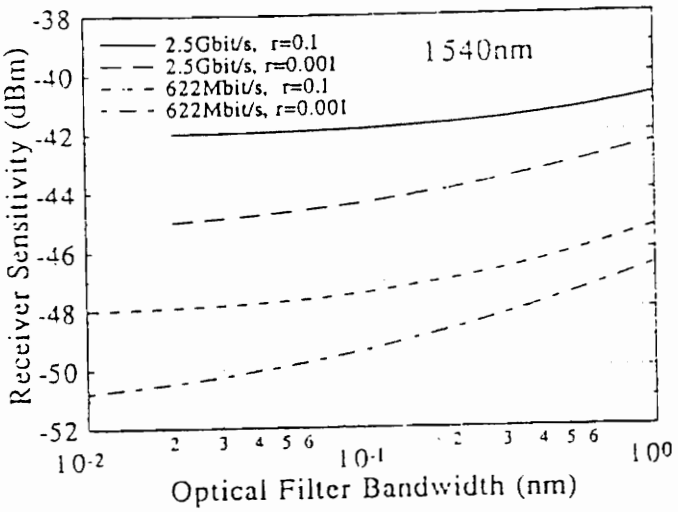


Fig. 4.12 Published results for receiver sensitivity (dBm) vs. optical filter BW for 622 Mb/s and 2.5 Gb/s for different extinction ratios 'r' [8]

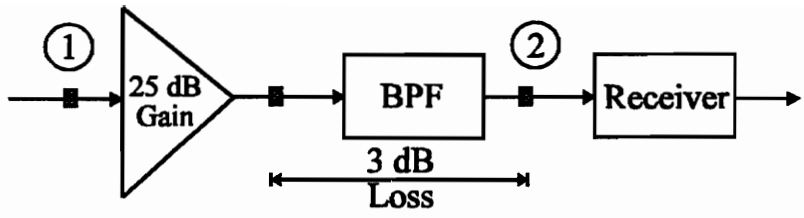


Fig. 4.13 Block diagram of the receiver used in [8]

From Fig. 4.12, the signal power ($P_S$) at stage 1 is -42.5 dBm, and the corresponding signal power at stage 2 is -20.5 dBm or 8.9 μW. The ASE power at stage 2 can be calculated by:

$$P_{ASE} = 2n_{sp}hf(G-1)$$

$$2n_{sp} = 3.4\ dB = 2.19; \quad hf = 1.293\times10^{-19}\ J; \quad G-1 = 315.23 \tag{4.17}$$

$$\therefore \text{At stage 2 without a polarization filter } P_{ASE} = 5.64\mu W$$

Next the baseline parameter 'b' is calculated from the given system parameters in [8]:

$$\text{Quantum Efficiency} = \eta = 0.8; \quad \text{Responsivity} = \frac{hq}{hf} \quad \therefore R = 0.99 \ \frac{A}{W};$$

$$b = \frac{kTB_e}{Z_e M^2 R^2}; \quad M = 10; \quad B_e = 1.5\left(\frac{2.48832\times10^9}{2}\right) Hz \tag{4.18}$$

$$\left(\frac{kT}{Z_e}\right)^{1/2} = 5\frac{pA}{\sqrt{Hz}}; \quad \Rightarrow \quad b = 4.783\times10^{-16}\ W^2$$

The sensitivity is not given, hence sensitivity of -27 dBm is assumed for this receiver at a BER of $10^{-12}$. By substituting the value of b and the sensitivity into Equation 4.14, the calculated value of a = $4.03\text{x}10^{-8}$. Note that these calculated values of a and b, are within

an order of magnitude of the values of the APD used in our experiments. Next we substitute the values of these parameters into our model:

$$m = BT = \left(\frac{1}{R_b}\right)\left(\frac{BW_{Optical}}{\lambda} * f\right) = 101.67$$

$$\kappa = \frac{2P_s\sqrt{m}}{\sqrt{P_{ASE}(P_{ASE}+4P_S)+4m(b+aP_s)}+\sqrt{P_{ASE}^2+4bm}} \tag{4.19}$$

$$\kappa = \frac{1.79\times10^{-4}}{1.95\times10^{-5}+5.66\times10^{-6}} = 7.14$$

Since kappa of 7 corresponds to a BER of $10^{-12}$, the error between the models is (7.14 - 7) 0.14. Eventhough the models are derived in different ways the results are similar. There are two differences that can be pointed out:

- The model presented here does not consider the penalties due to extinction ratios, while the model in [8] does.
- The model presented here does not consider the spontaneous shot noise, while the model in [8] does.

In conclusion, the model presented here can predict fairly accurately the BERs for different optical bandwidths and signal levels. This model has stood the test of extensive experimental results, and published theoretical results.

## 4.4 SOURCES OF ERRORS

The tunable filter used for these experiments consisted of two 10 nm filters. To calibrate the filter bandwidth, overlap of the two filters was monitored on the OSA assuming ASE has a flat spectrum. But the ASE spectrum is not absolutely flat, and hence the bandwidth measurement might be erroneous and introduce errors when comparing with the calculated results.

As mentioned in Section 4.3.2 this model does not account for spontaneous shot noise. ASE noise has a uniformly varying magnitude, which is transformed into a Poissonly varying noise current by the photodetector. This we feel is negligible and is not accounted for in the analysis.

In practical systems an attenuator will not be present between the pre-amplifier and the receiver as shown in Fig. 3.1. Rather a set-up as displayed in Fig. 4.13, where the output of the optical amplifier is filtered and passed directly to the receiver, is more practical. The motivation for placing the second attenuator was to keep the power into the amplifier constant (to generate fixed ASE) while studying the influence of bandwidth on the BER. It was not realized during the experiments that the attenuator makes analysis more complicated. As we discussed in Section 4.2, for a cascade of amplifiers the overall performance is dictated by the first stage if the first stage has high gain. But the second attenuator in Fig. 3.1 reduces and actually varies the gain of the first stage and shifts the importance to the receiver (second stage). This forced us to thoroughly model the receiver, and also reduced the possible improvement offered by the preamplifier. Summarizing, the second attenuator will not be used in practical systems and made the

analysis more complicated than was necessary. On the other hand, it enabled us to model a receiver in which there is a multiplicity of noise sources, not just ASE.

## 5.0 EFFECTS OF LASERS CENTER WAVELENGTH VARIATION

As shown in the previous chapter, the performance of an EDF pre-amplified system is strongly influenced by the optical bandwidth of the amplifier and the filter. The smaller the bandwidth, the lower the ASE noise allowed into the receiver; hence lower the sp-sp beat noise and better the performance. The limiting case for this argument is to make the filter bandwidth the same as the modulated laser spectral width. This filter would pass the signal and the ASE under the signal's spectral width and provide optimal performance. But as the filter bandwidth decreases, the system becomes highly sensitive to slight fluctuations in the laser's center wavelength. In the worst case, the laser might deviate out of the filter bandwidth, and the receiver would only see the ASE noise, ruining the BER performance. A laser can deviate due to temperature changes, and/or due to aging. With aging of the laser, the output power might decline and the driver circuit would increase the current to maintain a constant optical power and thereby change the wavelength of the

laser. This establishes a tradeoff between the system's sensitivity to slight changes in the laser wavelength and the performance. For a larger BW, larger variations in the laser's wavelength can be tolerated, but at the expense of poorer performance. On the other hand, a smaller BW gives a better performance but is highly sensitive to slight fluctuations. This suggests that in the presence of fluctuations there may be an optimal filter bandwidth.

To predict the degradation in performance, the following parameters must be considered: optical BW of the receiver, the filter's magnitude response, the spectral width of the laser, and typical fluctuations in wavelength over the lifetime of the laser. This chapter deals with the following issues: the first section contains a simple model to calculate the penalties, and receiver sensitivity based on filter characteristics. The following section gives the experimental results and compares them with the theoretical results.

## 5.1 A MODEL TO CALCULATE THE PENALTIES

Any bandpass filter ideally should have a pulse shaped magnitude response. The signals in the passband would experience a flat response, and the signals in the stopband are not allowed to pass. But real filters have a roll off, or transition bands, and stop bands offer a minimum amount of attenuation. Cosine roll off filters, may be used to model filters with small intersymbol interference [9]:

$$M(f)=\begin{cases} T & 0 \le |f| \le \dfrac{(1-\alpha)}{2T} \\ \dfrac{T}{2}\left[1-\sin\left(\dfrac{\pi T}{\alpha}\left[f-\dfrac{1}{2T}\right]\right)\right] & \dfrac{(1-\alpha)}{2T} \le |f| \le \dfrac{(1+\alpha)}{2T} \\ 0 & \dfrac{(1+\alpha)}{2T} \le |f| \end{cases} \qquad (5.1)$$

where 1/T is the full width half maximum (FWHM) bandwidth, and $\alpha$ is the roll off factor which controls the transition bands of the filter. An $\alpha$ of 0 represents no transition bands (Fig. 5.1), while an $\alpha$ of 1 allows for wide transition bands, with a gradual cutoff (Fig. 5.1). It is more convenient to work in the wavelength than in the frequency domain, and we will assume that the spectral shape in the wavelength domain may be approximated by the cosine roll-off shape.

$$M(\lambda)=\begin{cases} 1 & 0 \le |\lambda| \le \dfrac{B(1-\alpha)}{2} \\ \dfrac{1}{2}\left[1-Sin\left(\dfrac{\pi}{B\alpha}\left[\lambda-\dfrac{B}{2}\right]\right)\right] & \dfrac{B(1-\alpha)}{2} \le |\lambda| \le \dfrac{B(1+\alpha)}{2} \\ 0 & \dfrac{B(1+\alpha)}{2} \le |\lambda| \end{cases} \qquad (5.2)$$

In Equation 5.2, B represents the FWHM bandwidth (in units of wavelength). The response is normalized to have unity gain (0 dB) in the pass band.

In an ideal case the center laser wavelength is in the middle of bandpass filter and the entire signal is passed without any attenuation. Now let's assume the laser deviates and there is an offset between the center of the BPF and the laser center wavelength given by $\delta\lambda$ as shown in Fig. 5.2. Let's assume the laser has a finite spectral width given by $2\Delta\lambda$, and a rectangular power spectral density (PSD). A triangular PSD can also be easily accounted for, and will behave similarly. In an ideal situation, the laser's center wavelength will be aligned with the center of the BPF or $\delta\lambda = 0$, then the offset penalties would be zero. For a given offset and spectral width, the signal will be attenuated and introduce an optical power penalty. To analytically calculate the penalty, one can integrate the area under the laser's spectrum, and compare with the ideal case. This is done numerically (see Appendix 2), by first calculating the magnitude response of the filter with a given bandwidth and $\alpha$. A laser with a spectral width of $2\Delta\lambda$ is overlaid on the filter's magnitude response with an offset of $\delta\lambda$. A numerical integration is used to calculate the area under laser's spectral width.

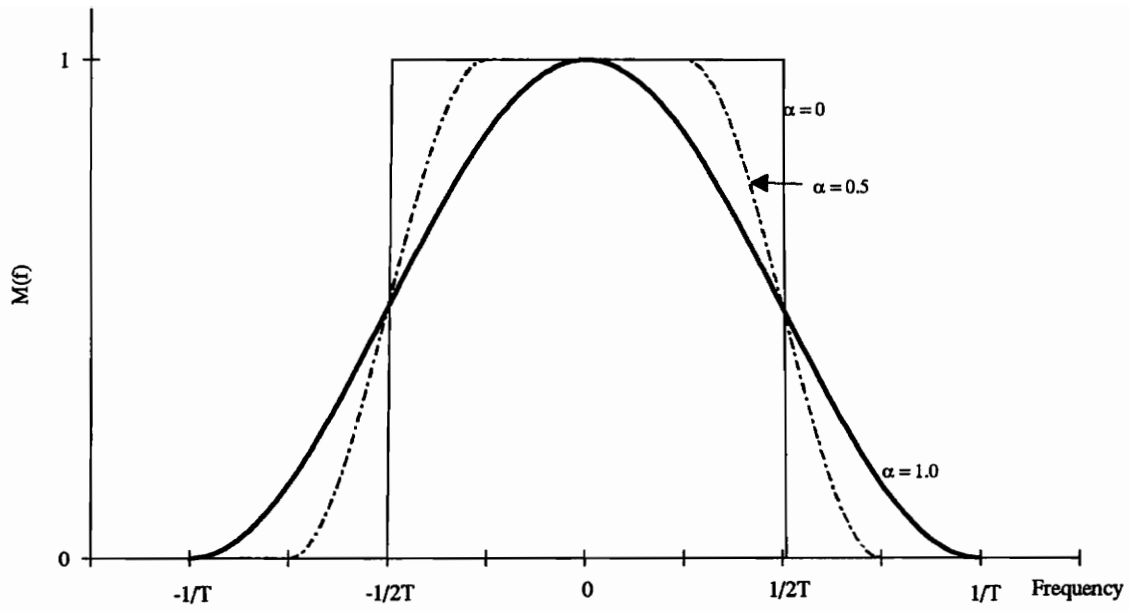


Fig. 5.1 Magnitude response of raised cosine roll-off filter

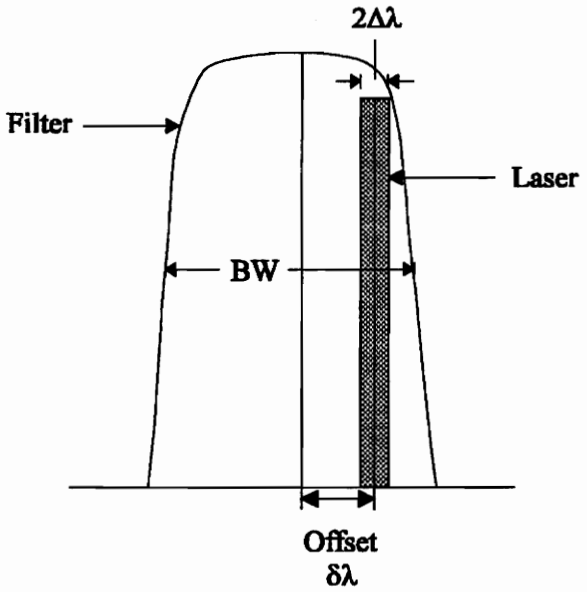


Fig. 5.2 Laser and filter spectra with offsets

Let ε be a normalized quantity given by:

$$\varepsilon = \frac{Offset}{Optical\ Bandwidth} = \frac{\delta\lambda}{B} \tag{5.3}$$

Let's assume that a laser's lifetime wavelength variations are going to be under 0.5 nm, while the laser's linewidth is 0.8 nm. The calculated penalties for various bandwidths are shown in Fig. 5.3 for α ranging from 0.1 to 1.0. The X-axis is epsilon, where an ε of 0.1 represents a BW of 5 nm with an offset of 0.5 nm, while an ε of 0.4 corresponds to a bandwidth of 1.25 nm. The Y-axis displays the penalty in dB, which is a ratio between the ideal case with no offsets to the area under the laser's spectral width with a given offset. As mentioned earlier for a constant offset, the smaller the bandwidth, the larger will be the penalty. This is demonstrated in Fig. 5.3, where the penalties are small at lower ε, but as ε increases (or the BW decreases) the penalties increase. Recall that for a given offset, the smaller bandwidths provide better performance but are sensitive to the offset penalties.

Fig. 5.3 displays penalties for α ranging from 0.1 to 1.0. The value of ε at the knee of the curves increases as the value of α decreases. For a smaller α, a smaller bandwidth is sufficient to accommodate the laser, hence the penalties are noticeable at higher values of ε. After the knee of the curve, for $\alpha \approx 0$ the rate of degradation of performance is rapid. This is because once the bandwidth of the filter is narrower than the spectral width of the laser, the power captured by the filter decreases and the penalty becomes large. On the other hand, for larger values of α the passband is small for the same bandwidth, hence the knee of the curve occurs at larger bandwidths or smaller ε. For $\alpha \approx 1$, even though the

penalties start at the smaller values of ε, the slope of the curve (Fig. 5.3) is not as steep and the degradation of the performance is not as rapid.

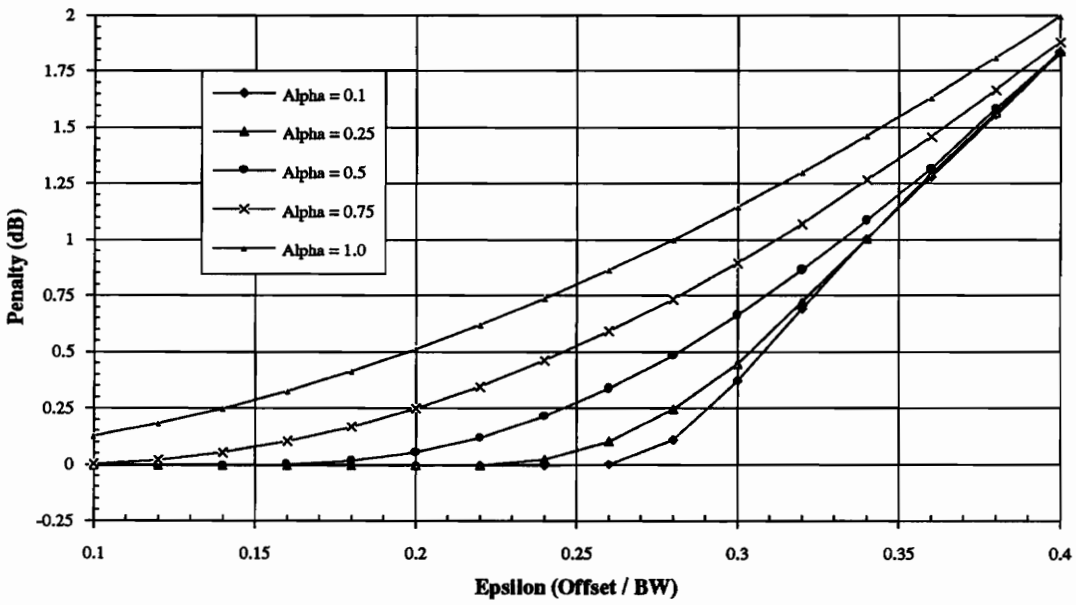


Fig. 5.3 Optical power penalty (dB) vs. epsilon for $\alpha = 0.1$ to 1.0

Summarizing, for a fixed offset the smaller bandwidths experience a higher penalty. Filters with small bandwidths and small $\alpha$, can be used to provide good performance but after the threshold the degradation of performance is rapid. Overall, the larger values of $\alpha$ provide poorer performance than the smaller values of $\alpha$.

Next, we examine the effect of these penalties on the receiver sensitivity. Most fiber optic communication systems are designed to provide a BER of $10^{-9}$ (kappa = 6). The signal power (Ps) required to meet the above criteria is called the receiver sensitivity. Sensitivity can also be expressed in terms of Number of Photons/Bit (Np) required to meet a performance criteria, and is expressed as:

$$N_P = \left(\frac{P_s}{hf}\right)\left(\frac{1}{R_b}\right) \equiv \left[\frac{J}{Sec.}\right]\left[\frac{Photon}{J}\right]\left[\frac{Sec.}{Bits}\right] \equiv \left[\frac{Photons}{Bit}\right] \tag{5.4}$$

where $R_b$ is the bit rate, and hf is the energy in a signal photon. Sensitivity was derived in [7] to be:

$$N_P = 2n_{sp}\kappa\frac{G-1}{G}\left[\kappa + \sqrt{0.75B_{Hz}T + \left[\frac{N_1}{\kappa n_{sp}(G-1)}\right]^2}\right] \tag{5.5}$$

The second term inside the square root sign accounts for the thermal noise, which is negligible for an APD receiver. In Equation 5.5, $B_{Hz}$ is the optical bandwidth in Hertz of the amplifier, and T is the bit period. Furthermore, for a high gain optical amplifier (G > 15 dB) (G-1/G) $\approx$ 1, hence Equation 5.5 simplifies to:

$$N_P = 2n_{sp}\kappa\left[\kappa + \sqrt{0.75B_{Hz}T}\right] \tag{5.6}$$

For a low noise EDFA the value of $n_{sp}$ can be as low as 2. As mentioned earlier, BER of $10^{-9}$ corresponds to $\kappa = 6$. Let's work with a data rate of 2.5 Gb/s, and a laser operating at 1546.9 nm. Using these assumptions Equation 5.6 reduces to:

$$B_{Hz} = \left[\frac{B(nm)}{1546.9}\right]\left[\frac{3\times10^{8}}{1546.9\times10^{-9}}\right] \quad Hz \Rightarrow B_{Hz}T = 50.38B \tag{5.7}$$

$$\therefore \quad N_P = 24\left[6 + \sqrt{37.788B}\right]$$

Here we have assumed that the laser is centered within an optical filter with a bandwidth of B nm. Equation 5.7 can be used to theoretically predict the receiver sensitivity at various bandwidths, as shown in Fig. 5.4. The X-axis is the optical bandwidth in nm, and the Y-axis is the receiver sensitivity in number of photons/bit. Note that as the BW increases, so does the signal power required to provide a BER of $10^{-9}$, which translates into a poorer sensitivity and performance.

Now let's introduce the penalties due to offsets and rewrite Equation 5.7 as:

$$N_P = 24\left[6 + \sqrt{37.788B}\right].Penalty(ratio) \tag{5.8}$$

$$Penalty \equiv \frac{Area\ under\ the\ laser(Ideal\ Situation)}{Area\ under\ the\ laser\ \&\ filter\ with\ offset}$$

Here penalty is the ratio of the signal power seen at the output of the filter with no offset when compared to the power at the output of the filter with an offset. This ratio will

always be ≥ 1, and results in an increase in the number of photons/bit required to provide a BER of $10^{-9}$. Using Equation 5.8, we consider the same scenario as in Fig. 5.3, i.e. an offset of 0.5 nm, and laser linewidth of 0.8 nm and vary the bandwidth to see the effect on the sensitivity of the system. In Fig. 5.5, the X-axis is ε (offset/BW) and Y-axis is the number of photons/Bit to provide $10^{-9}$ BER for $\alpha$=0.25.

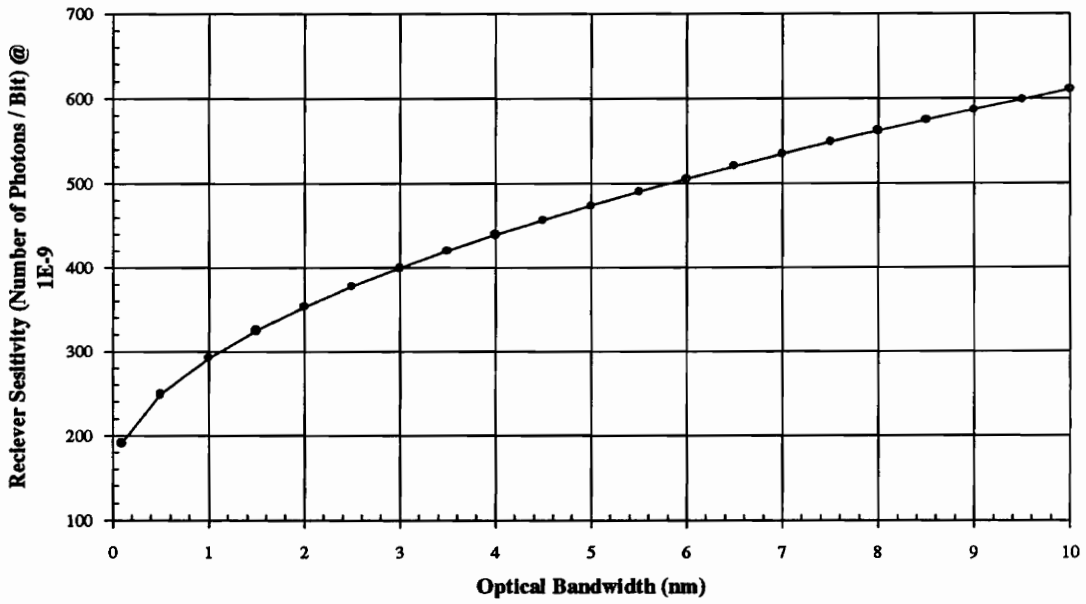


Fig. 5.4 Calculated receiver sensitivity vs. optical bandwidth

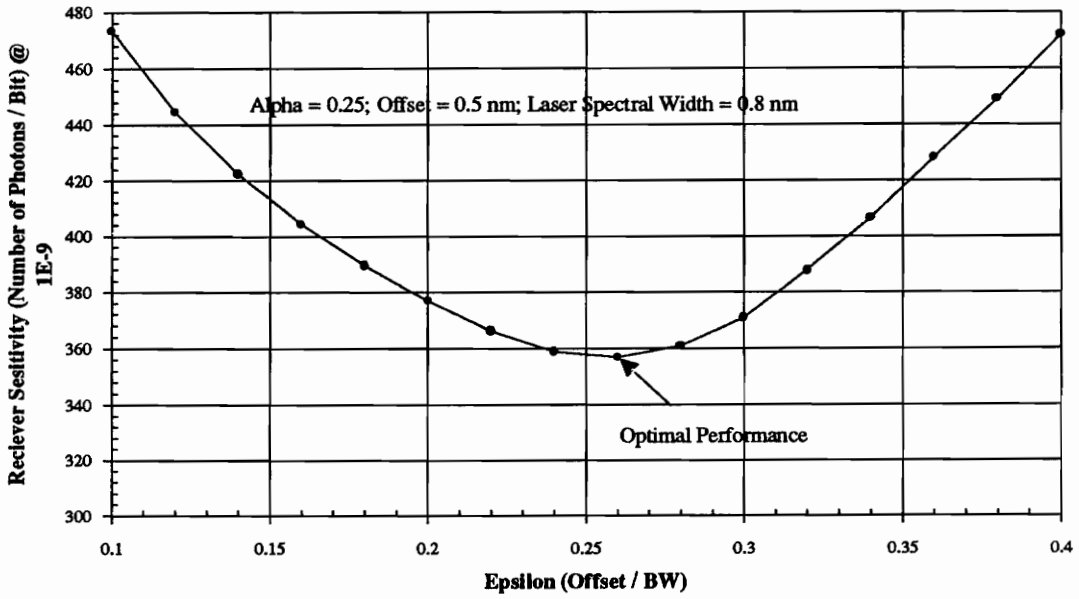


Fig. 5.5 Receiver sensitivity vs. epsilon for $\alpha = 0.25$

Note that as ε starts increasing from 0.1 the sensitivity improves and reaches an optimal point at ε = 0.26, and degrades for higher values of ε. This can be explained by noticing that as ε increases the bandwidth decreases, which translates into an improved performance as shown in Fig. 5.4. But a drastic reduction in the bandwidth for a given offset introduces optical penalties, accounted by the second term in Equation 5.8, and the relative improvement in the sensitivity due to the decrease in bandwidth is lost. The domination of second term (in Equation 5.8) translates into poorer performance and hence the upturn in the curve. Summarizing, there exists an optimal ε, which yields the best sensitivity for a given offset. At the point of optimal performance, there exists a balance between the improvements in performance and penalties due to the reduction in bandwidth.

The optimal value of ε is a function of α which we discuss next. Fig. 5.6 plots the sensitivity in number of photons/bit as a function of ε for α ranging from 0.1 to 1.0. When comparing this curve to Fig. 5.5 two observations can be made about the point of optimal performance:

- As α increases from 0.1 to 1.0, the curve becomes flatter, i.e., is less strongly dependent on ε. This is due to the penalties term in Equation 5.8. Note that when $\alpha \approx 1$, the filter magnitude response is smooth and the transition bands are wide. Therefore, as epsilon changes, the effect on performance is gradual but not significant. For $\alpha \approx 0$ the improvement with the increase in ε is rapid, due to the removal of ASE until the optimal performance is achieved. But after the point of optimal performance, the degradation in performance is rapid due to the sharp transition bands, and the slope of the curve is high.

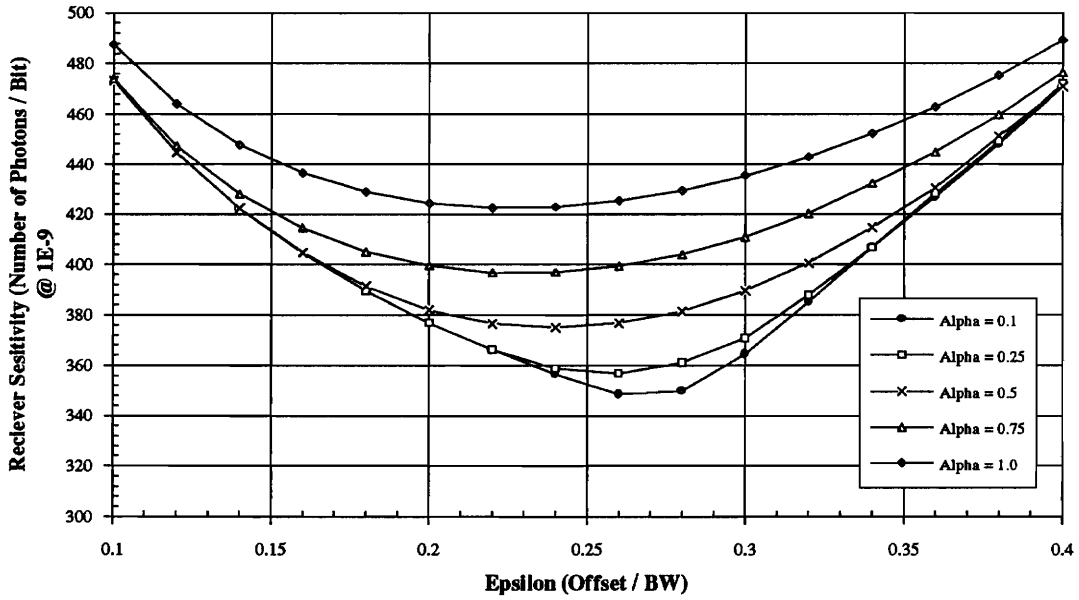


Fig. 5.6 Receiver sensitivity vs. epsilon for $\alpha = 0.1$ to 1

However, for $\alpha \approx 1$, even though the overall performance is poorer, the decline in performance at higher epsilon is more gradual.

- A second point of interest is the value of epsilon where the optimal performance occurs in Fig 5.6. A higher optimal value of $\varepsilon$ is observed for smaller values of $\alpha$. Recall, that the higher value of $\varepsilon$ correspond to the smaller bandwidths, implying that a smaller $\alpha$ provides better sensitivity at smaller bandwidths. Since the pass band is wider for a smaller $\alpha$, a smaller BW can accommodate the laser without introducing any penalties. But for larger values of $\alpha$ the passband is smaller (for the same bandwidth), and the transition band is wider, hence the penalties are noticeable at smaller values of $\varepsilon$ (or larger bandwidths).

Fig. 5.6 provides a designer with the freedom to design the $\alpha$ and the bandwidth of the filter to meet the given requirements. An optimal bandwidth can be selected taking into account the expected variation in laser's center wavelength. As shown in Fig. 5.5, an $\varepsilon$ = 0.26 gives optimal performance for the given parameters. This $\varepsilon$ translates into the following optimal bandwidth for an offset of 0.5 nm:

$$B = \frac{Offset}{\varepsilon} = \frac{0.5}{0.26} = 1.92\ nm \approx 2\ nm \tag{5.9}$$

From Fig 5.6 we obtain the following values of $\varepsilon$ that yield the optimal performance (for an offset 0.5 nm) for various values of $\alpha$:

Table 2: Optimal bandwidth for various values of $\alpha$

| $\alpha$ | Optimal $\varepsilon$ | BW (nm) |
|---|---|---|
| | | |
| 0.1 | 0.26 | 1.92 |
| 0.25 | 0.26 | 1.92 |
| 0.5 | 0.24 | 2.08 |
| 0.75 | 0.22 | 2.27 |
| 1 | 0.22 | 2.27 |

Note that the optimal range of $\varepsilon$ ranges from 0.22 to 0.26. As a rule of thumb, system designers can multiply the expected offset over the lifetime of the laser by 4 to derive the optimal bandwidth.

Summarizing, smaller bandwidths with smaller values of $\alpha$ provide better performance in ideal cases. But after the point of optimal performance, the performance deteriorates rapidly with increase in epsilon (decrease in bandwidth) due to accrued penalties. Whereas larger bandwidths with larger values of $\alpha$ provide poorer overall performance in ideal scenarios, they do not show as rapid a degradation with increased epsilon.

## 5.2 MEASURED RESULTS

In this section we look at the measured performance with offsets. The experimental set-up in Fig. 3.1 was also used for this portion of the experiments. To simulate variation in signal wavelength, the center of the optical BPF was offset with respect to the laser center wavelength, creating the same effect as shown in Fig. 5.2. To calibrate the filter

bandwidth and offsets, the wideband ASE noise and signal were observed on the OSA and the filters tuned. This was not a very exact calibration, for two reasons: (1) the offsets with respect to the center of the filter cannot be measured exactly, and (2) ASE doesn't have a flat PSD and variations in the PSD could be mistaken for the filter characteristics. In this section, instead of focusing on the exact numbers, we will focus on the relative differences and compare with the behavior predicted in the previous section. Let's look at three graphs to fully understand and observe the influence of offsets on penalties:

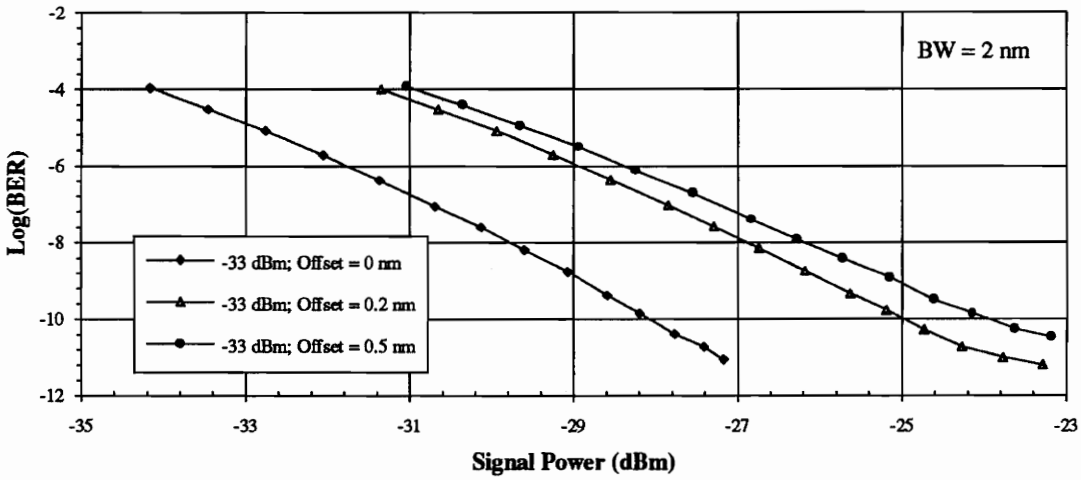


Fig. 5.7 Signal power vs. log(BER) for 2 nm filter with 0, 0.2, and 0.5 nm offsets

Fig. 5.7 is a graph of log of BER vs. the signal power, with a 2 nm filter and -33 dBm into the pre-amplifier. This graph plots data for three offset settings: without any offset, and with 0.2 nm and 0.5 nm offsets. The BER performance degrades severely with a 0.2 nm variation in laser center wavelength. However, an additional variation of 0.3 nm generates minor degradation in performance. This is counter intuitive and cannot be explained by the simple model in section 5.1. This we believe is due to the calibration errors explained earlier.

Recall that for a small filter bandwidth, the BER performance is highly susceptible to slight changes in the center wavelength. This is evident in Fig. 5.7, where ~ 4 dB penalty is encountered at a BER of $10^{-9}$ with offsets ≤ 0.5 nm.

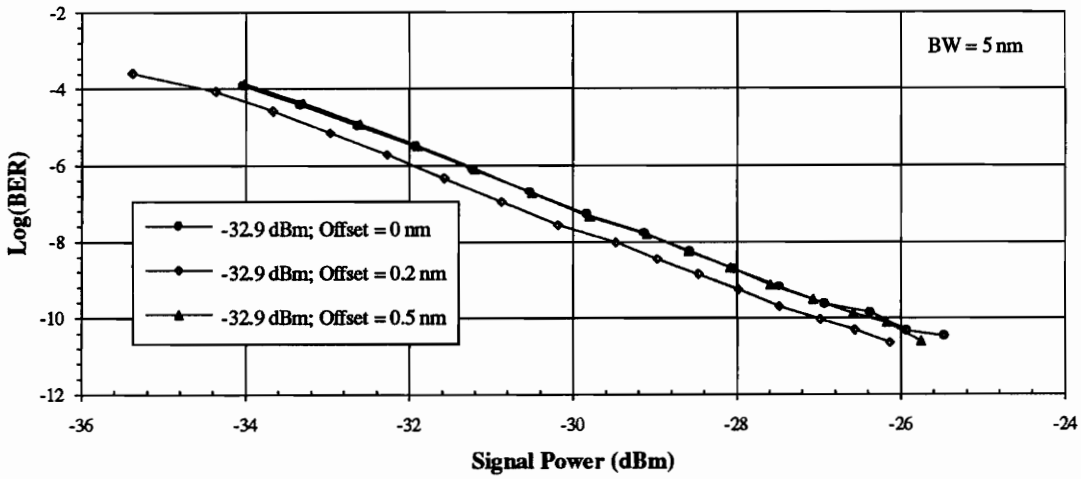


Fig. 5.8 Signal power vs. log(BER) for 5 nm filter with 0, 0.2, and 0.5 nm offsets.

Fig. 5.8 is a graph of log of BER vs. signal power for a 5 nm filter and -33 dBm signal power into the EDFA. This graph uses exactly the same parameters as the previous graph, except the filter bandwidth, but yields different results. Firstly, the sensitivity of the 2 nm filter without an offset is -29 dBm, and the sensitivity with a 5 nm filter is -28 dBm. As expected the 2 nm filter, out performs the 5 nm filter in an ideal case (no offsets). Even though the 5 nm filter yields a poorer sensitivity, the offsets barely effect the performance (within experimental errors). As seen from this graph, with 0.2 nm and 0.5 nm offsets the degradation of performance is minimal and the three curves cluster together. Note that 0.2 nm offset curve out performs the curve without any offset. This cannot be explained by our model, but rather is likely due to the calibration errors.

The BER performance with the 5 nm filter is more robust to offsets than the 2 nm filter results displayed in Fig. 5.7. As mentioned in the previous section, for a wide bandwidth the performance is relatively insensitive to the offsets, and the degradation in the performance is minimal.

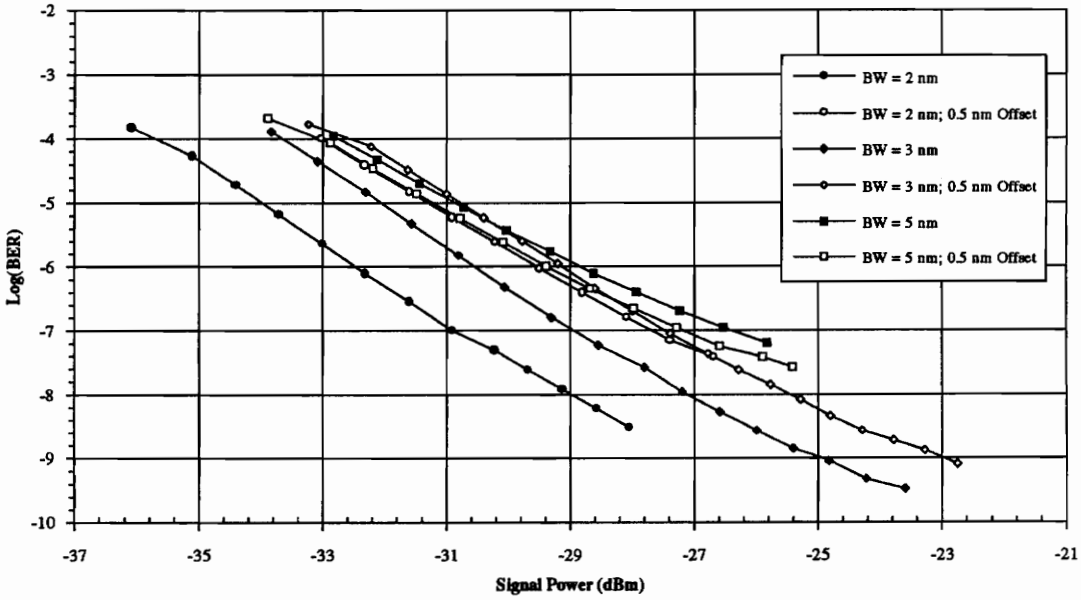


Fig. 5.9 Signal power vs log(BER) for 2, 3, & 5 nm filters with & without offsets.

Fig. 5.9 is a graph of log of BER vs. the signal power for 2, 3, and 5 nm bandwidths with and without a 0.5 nm offset for -35 dBm into the EDFA. As would be expected, a 2 nm filter out performs both the 3 and 5 nm filters without the offsets. Although the 2 nm filter offers the best performance under ideal conditions, its sensitivity to small offsets result in severe degradation of performance. The 3 nm filter shows a smaller degradation with a 0.5 nm offset, and the 5 nm filter has an even smaller degradation. With the 0.5 nm offset

the 2, 3, and 5 nm filters offer almost the same performance (within experimental errors) and the relative improvement offered by the 2 nm filter is wiped out.

Summarizing, experimentally we have shown that even though smaller bandwidth filters out perform the wider bandwidth filters in ideal scenarios, they are highly sensitive to slight fluctuations in the laser's center wavelength. We have also shown that with offsets, a wider bandwidth filter yields comparable performance to a smaller bandwidth filter, and the anticipated improvements from the smaller bandwidth filter are not realized. The results are in qualitative agreement with our theoretical model, but likely calibration errors make quantitative comparison difficult.

As an alternative to predicting the offset penalties and choosing the optimal filter bandwidth, a self tuning BPF which tracks the laser can be used. A scheme was suggested by JDS Fitel, a manufacturer of optical components, where a tunable filter has two output ports, one for through transmission and the other for monitoring the signal. Offset penalties can be removed by using optics to monitor the drift of the laser, and then tuning the filter such that the laser always remains in the center of the filter. From a telephone conversation with Joe Ip of JDS Fitel [10], we understand that the filter for EDFA applications would cost around ten thousand dollars and the monitoring and controlling hardware will be additional. We believe there are two disadvantages of this filter today, (1) this scheme is very expensive and (2) another complicated component is added to the receiver, and raises additional reliability issues. Therefore, a passive filter is the practical choice for pre-amplified receivers of today.

# 6.0 CONCLUSIONS

In this thesis we have studied the influence of filter characteristics, principally bandwidth, on the BER performance of an EDF pre-amplified APD receiver.

Although an EDFA can amplify optical signals independent of the information, data rates, or modulation schemes, the EDFA adds a wideband ASE noise. The bulk of the ASE power is removed with an optical BPF following the EDFA, and doesn't enter the receiver. The smaller the bandwidth of the BPF, the lesser the ASE allowed into the receiver, hence the better the performance. We have derived a model that predicts the BER performance for given APD parameters, and filter bandwidths. This model takes into account the sp-sp, and sig-sp beat noises generated by the square law action of the photodetector. This model also includes the signal-shot, and thermal noises generated by the receiver. We have compared the predicted performance and the measured results for various

bandwidths, and signal levels. The discrepancies between the measured and predicted results could be caused due to the saturation of the receiver, or signal dependent noise sources, or errors in bandwidth and power measurements. There is general agreement between the measured and the calculated results, and we have not discerned a systematic difference between the measurements and the model. The model was also compared with theoretical results published by Ruhl and Ayre in [8]. Even though the authors of [8] used different models and assumptions, a close match between the two results was observed.

Ideally, a filter bandwidth the same as the modulated spectral width of the laser would select the signal and a small portion of the ASE spectrum, and yield the best performance. But as the filter bandwidth decreases, the system becomes highly sensitive to slight fluctuations in the laser's center wavelength. We have modeled an optical BPF using a cosine roll-off wavelength response, and predicted the optical penalties as the laser wavelength changes. We have demonstrated that the penalties are a function of the filter BW, the filter roll-off factor, the laser spectral linewidth, and the offset between the center of the BPF and the laser spectrum. We have also determined and demonstrated that a filter bandwidth about four times the expected laser wavelength variation will yield the optimal performance. Although, a filter with sharp roll-off and small bandwidth provides good performance, the degradation of performance is rapid for laser wavelength offsets when the roll off is more gradual. Although a filter with a more gradual roll-off and wider bandwidth provides poorer performance, it is more robust to slight variation in the laser wavelength. This behavior establishes a tradeoff between the performance of the system and the sensitivity to slight variation in the wavelength.

Summarizing, characteristics of the BPF are crucial parameters for a optically pre-amplified receiver. It determines the performance and the stability of the communication link.

## 6.1 FUTURE DIRECTIONS

There are several additional ways in which the data in this thesis may be used. For example, recently there has been debate over how to measure the spontaneous emission factor ($n_{sp}$) of an optical amplifier. $n_{sp}$ is directly proportional to the ASE noise power, and is crucial for the characterization of the amplifier. Today we can measure the power in an optical signal by converting it to an electrical signal. The opto-electric conversion and processing corrupts the original optical signal by the addition of shot and thermal noise terms. We plan to use the model in Equation 4.12, and the measured values of kappa, to determine $P_{ASE}$ while keeping all other parameters the same. Since the model successfully characterizes the APD receiver, and can accurately predict the shot and thermal noise terms, therefore it will allow us to estimate $P_{ASE}$. Using the estimated value of $P_{ASE}$, and other parameters like the bandwidth, and energy of a signal photon the value of $n_{sp}$ can be calculated. This can then be compared with the $n_{sp}$ obtained from our direct measurements of $P_{ASE}$.

# References


[1] Emmanuel Desurvire, "Lightwave Communications: The Fifth Generation," *Scientific American*, January 1992.

[2] Emmanuel Desurvire, "Basic Physics erbium-Doped Fiber Amplifiers," Center for Telecommunications Research, Department of Electrical Engineering, Columbia University. Department of Electrical Engineering, 500 W. 120th Street, New York, NY 10027. Published in 1991.

[3] TM-TSV-021435, July 1991, "Optical Fiber Amplifier Performance Characterization," Bellcore IEM, 445 South Street, Room 2J125, Morristown, NJ 07962.

[4] N. A. Olsson, Lightwave Systems with Optical Amplifiers," *Journal of Lightwave Technology*, Vol. 7, No. 7, pp. 1071-1082, July 1989.

[5] Ozan K. Tonguz, and Leonid G. Kazovsky, "Theory of Direct-Detection Lightwave Receivers Using Optical Amplifiers," Journal of Lightwave Technology, Vol. 9, No. 2, pp. 174-181, February 1991.

[6] William B. Jones, "Introduction to Optical Fiber Communication Systems," Holt, Reinhart and Winston, Inc 1988.

[7] Ira Jacobs and Bechara Raad, "Receiver Sensitivity of Lightwave systems using optical amplifiers," in CLEO '91 Baltimore, MD. May 1991.

[8] F.F. Ruhl and R.W. Ayre, "Explicit Expressions for the Receiver Sensitivity and System Penalties of Optically Preamplifed Direct-Detection Systems," *IEEE Photonics Technology Letters*, Vol. 5, No. 3, pp. 358-361, March 1993.

[9] John G. Proakis, "Digital Communications," 2nd Edition, McGraw Hill in Electrical Engineering, 1989

[10] Telephone conversation with Joe Ip of JDS Fitel on June 10, 1993. JDS Fitel, 570 Heston Drive, Nepean, Ontario Canada. Phone No. (613) 727-1303

[11] TM-TSV-021692, October 1992, "Impacts of Optical Bandpass Filter Characteristics on erbium Doped Fiber pre-Amplifier System Performance," Bellcore IEM, 445 South Street, Room 2J125, Morristown, NJ 07962.

# Appendix 1

$$BER = Q(\kappa)$$

$$\text{where} \quad Q(\kappa) = \frac{1}{\sqrt{2\pi}} \int_{\kappa}^{\infty} e^{-x^2/2} dx$$

| κ | BER | κ | BER |
|---|---|---|---|
| | | | |
| 2.15 | 1.6E-02 | 4.7 | 1.3E-06 |
| 2.3 | 1.1E-02 | 4.85 | 6.2E-07 |
| 2.45 | 7.1E-03 | 5 | 2.9E-07 |
| 2.6 | 4.7E-03 | 5.15 | 1.3E-07 |
| 2.75 | 3.0E-03 | 5.3 | 5.8E-08 |
| 2.9 | 1.9E-03 | 5.45 | 2.5E-08 |
| 3.05 | 1.1E-03 | 5.6 | 1.1E-08 |
| 3.2 | 6.9E-04 | 5.75 | 4.5E-09 |
| 3.35 | 4.0E-04 | 5.9 | 1.8E-09 |
| 3.5 | 2.3E-04 | 6.05 | 7.2E-10 |
| 3.65 | 1.3E-04 | 6.2 | 2.8E-10 |
| 3.8 | 7.2E-05 | 6.35 | 1.1E-10 |
| 3.95 | 3.9E-05 | 6.5 | 4.0E-11 |
| 4.1 | 2.1E-05 | 6.65 | 1.5E-11 |
| 4.25 | 1.1E-05 | 6.8 | 5.2E-12 |
| 4.4 | 5.4E-06 | 6.95 | 1.8E-12 |
| 4.55 | 2.7E-06 | 7.1 | 6.2E-13 |

This table contains the kappa and the corresponding BER values. The graph displays that BER rolls off gradually at the lower values of kappa, but at the higher values of kappa the roll-off is steep. Receiver sensitivity is often specified at BER of $10^{-9}$, but much lower BER may be desired in actual system operation.

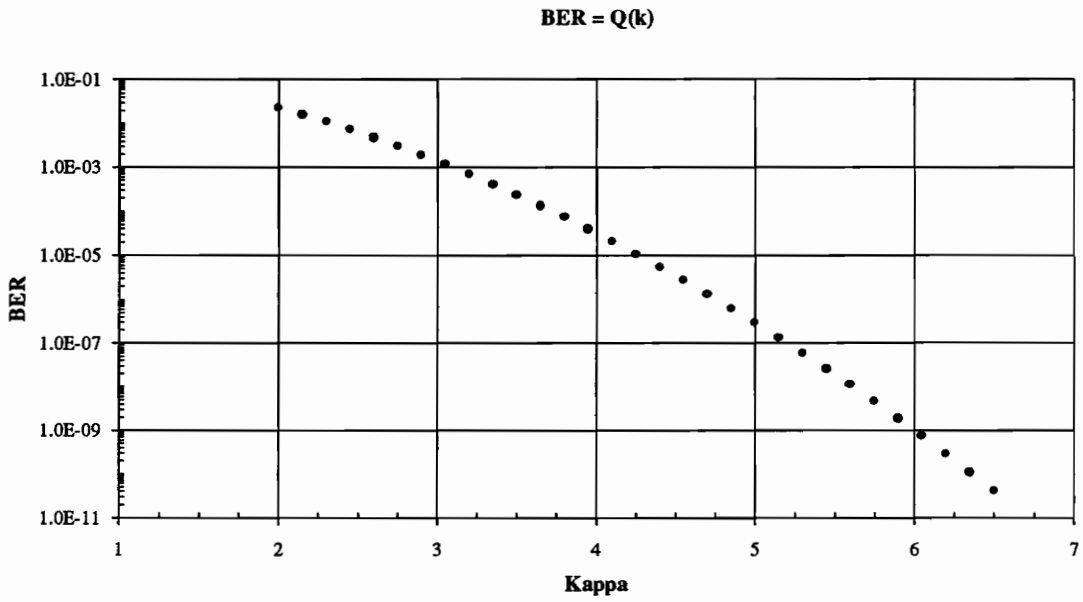
BER = Q(k)
1.0E-01
1.0E-03
1.0E-05
1.0E-07
1.0E-09
1.0E-11
BER
1
2
3
4
5
6
7
Kappa

# Appendix 2

```
% This Program calculates the penalties (in dB and ratios) and the receiver sensitivities for given
% values of α and the spectral width of the laser.

% offset = Offset between the laser's center wavelength and center of the filter;
% DL=Laser's Spectral Width;   eps = Epsillon (Offset / BW)      BW = Vector of filter bandwidths


clear;clc;

inc =0.001;  eps = [0.1:.02:.4];
offset = [0.25 0.5 1.0 1.5 2];

α = input(' Input the Roll Off Factor:  ');
DL = input(' Input the Full Spectral Width of the Laser:  ');

DL = DL/2;
nostep = floor((2*DL)/inc);

for j=1:length(offset)

        BW = offset(j)./eps;

        for k = 1:length(BW)

                [fil_resp, lamda] = cos_rol(α,BW(k));
                start = floor((BW(k) + offset(j) - DL)/inc);

                resp=0;
                for i = start:nostep+start
                        resp = resp + fil_resp(i);
                end

                pen(j,k) = nostep/resp;
                pen_db(j,k) = 10*log10(nostep/resp);
                sens(j,k) = 24*(6 + sqrt(37.788*BW(k)))*pen(j,k);

        end
end
```

# VITA

Vikas Hari Butaney was born in New Delhi, India in March 1970. He attended Sardar Patel Vidyalaya in New Delhi from Nursery till 11th Grade. In November 1986, he immigrated to America with his family and completed his high school at Langley High School in McLean, VA. After receiving his B.S. in Electrical Engineering in May 1991, from the Bradley Department of Electrical Engineering at VA. Tech, he worked for LCC as a Cellular Engineer. In January '92, he returned to VA. Tech to start his Graduate Studies under Dr. Ira Jacobs, with plans to focus on Optical Communications. In the summer of 1992, he had the golden opportunity to perform experiments and collect data at Bellcore in Red Bank, NJ. This thesis is a result of the work, and experiments at Bellcore. After graduation, he plans to work with Bell Atlantic Network Services in Fairfax, VA as a Systems Engineer, and perform system level design of data communication systems.